European Journal of Applied Mathematics (2026), **37**, pp. 1465–1486
doi:10.1017/S0956792526100370

CAMBRIDGE UNIVERSITY PRESS

PAPERS

Global Hopf bifurcation and connected components in a delayed predator–prey model

Wael El Khateeb[1], Guihong Fan[2], Chunhua Shan[1] and Hao Wang[3]

[1]The University of Toledo, USA
[2]Columbus State University, USA
[3]University of Alberta, Canada
Corresponding author: Hao Wang; Email: hao8@ualberta.ca

Received: 03 September 2025; **Revised:** 25 March 2026; **Accepted:** 25 March 2026; **First published online:** 22 April 2026

Keywords: Periodic solutions; global Hopf bifurcation; nested connected component; combined effects of delay and carrying capacity; Fuller's space

2020 Mathematics Subject Classification: 37N25 (Primary); 92D25 (Secondary)

Abstract

We study the dynamics of a delayed predator–prey system with Holling type II functional response, focusing on the interplay between time delay and carrying capacity. Using local and global Hopf bifurcation theory, we establish the existence of sequences of bifurcations as the delay parameter varies and prove that the connected components of global Hopf branches are nested under suitable conditions. A novel contribution is the demonstration that the classical limit cycle of the non-delayed system belongs to a connected component of the global Hopf bifurcation in Fuller's space. Our analysis combines rigorous functional differential equation theory with continuation methods to characterize the structure and boundedness of bifurcation branches. We further demonstrate that delays can induce oscillatory coexistence at lower carrying capacities than in the corresponding ordinary differential equation model, yielding counterintuitive biological insights. The results contribute to the broader theory of global bifurcations in delay differential equations while providing new perspectives on nonlinear population dynamics.

1. Introduction

In the early twentieth century, Lotka and Volterra pioneered the mathematical study of population dynamics, introducing models that remain central to theoretical ecology. Their work provided a foundational framework for describing predator–prey interactions and inspired a wide range of generalizations. A commonly studied form of the generalized Lotka-Volterra model is

$$\begin{cases} \dfrac{dx(t)}{dt} = x\alpha(x) - p(x)y, \\ \dfrac{dy(t)}{dt} = cp(x)y - dy, \end{cases} \tag{1.1}$$

where $x(t)$ and $y(t)$ denote the prey and predator densities at time t, respectively. Here, $\alpha(x)$ describes the per capita prey growth rate in the absence of predation, c is the conversion efficiency of prey into predator biomass, d is the predator mortality rate, and $p(x)$ is the functional response characterizing the predation rate as a function of prey density.

To capture the biological fact that prey consumption does not instantly translate into predator reproduction, a time delay τ is introduced. Specifically, τ represents the period between prey capture and its conversion into viable predator biomass. The survival probability of predators during this interval

© The Author(s), 2026. Published by Cambridge University Press. This is an Open Access article, distributed under the terms of the Creative Commons Attribution licence (https://creativecommons.org/licenses/by/4.0/), which permits unrestricted re-use, distribution and reproduction, provided the original article is properly cited.

https://doi.org/10.1017/S0956792526100370 Published online by Cambridge University Press

is given by $e^{-d\tau}$ [2]. Assuming logistic growth for the prey population and a Holling type II functional response, we obtain the delayed predator–prey system

$$\begin{cases} \dfrac{dx(t)}{dt} = rx(t)\left(1 - \dfrac{x(t)}{K}\right) - \dfrac{mx(t)y(t)}{a + x(t)}, \\ \dfrac{dy(t)}{dt} = -dy(t) + e^{-d\tau}\dfrac{cmx(t-\tau)y(t-\tau)}{a + x(t-\tau)}, \end{cases} \tag{1.2}$$

where r is the intrinsic prey growth rate, K is the environmental carrying capacity, a is the half-saturation constant, and m is the predation rate. All parameters are positive. The incorporation of τ renders the model more realistic by reflecting the maturation time of predators and compensating for mortality during the delay.

Such delayed predator–prey systems have been extensively studied from both biological and mathematical perspectives; see [5–7, 11, 15, 18, 20, 23, 26–28] and references therein. An alternative biological interpretation of the delay and survival term $e^{-d\tau}$ was proposed by Gourley and Kuang [7], who studied stage-structured models in which juvenile predators experience a mortality rate $d_j \neq d$ during the maturation period τ, leading to the survival factor $e^{-d_j\tau}$. Related stage-structured models with Holling type I and II responses were analysed by Gourley and Kuang [7] and by Li, Lin, and Wang [11] using Hopf bifurcation analysis. Cooke, Elderkin, and Huang [5] incorporated juvenile prey mortality into similar delayed systems, while Fan and Wolkowicz [6] considered model (1.2) with a Holling type I response, demonstrating the existence of local Hopf bifurcations and a cascade of period-doublings leading to chaos. Diffusive extensions with predator maturation delay have also been investigated, for instance by Xu et al. [28] in the context of global Hopf bifurcation. More broadly, delay has been employed in predator–prey models to capture diverse biological mechanisms and to explore their rich dynamical behaviour [4, 15, 18, 20, 21, 23, 26, 27].

It is well known that the corresponding ordinary differential equation (ODE) model obtained by setting $\tau = 0$ in (1.2) admits a unique globally asymptotically stable periodic orbit. The focus of this paper is to uncover the richer dynamics that emerge for $\tau > 0$, with particular emphasis on the global structure of Hopf bifurcation. Our main results are as follows:

- There exists a sequence of local Hopf bifurcations as τ (or K) varies. Under suitable conditions, the connected components of the global Hopf bifurcation are nested with respect to τ.
- The limit cycle of the ODE model belongs to a connected component of the global Hopf bifurcation of the DDE model (1.2) in Fuller's space. This connection between ODE periodic orbits and DDE Hopf components appears to be new.
- Introducing a positive delay τ can lead to predator–prey coexistence through oscillatory dynamics at lower carrying capacities compared to the delay-free case, a counterintuitive phenomenon given the mortality losses incurred during the delay.

The novelty of the second result lies in establishing a precise relationship between ODE limit cycles and global Hopf components in delay differential equations, which to the best of our knowledge has not been reported in the context of Holling-type functional responses. The third result offers new biological insight by demonstrating that delay can in fact facilitate coexistence under more restrictive environmental conditions.

The paper is organized as follows. In Section 2, we establish the well-posedness of (1.2) with prescribed initial data and recall the known dynamics of the corresponding ODE model. Section 3 analyses local dynamics near equilibria and the onset of Hopf bifurcations. Section 4 develops the theory of global Hopf bifurcation and connected components. In Section 5, we present bifurcation diagrams in the (τ, K)-plane, highlighting the joint effects of delay and carrying capacity. Section 6 concludes with biological interpretation and significance of the results.

https://doi.org/10.1017/S0956792526100370 Published online by Cambridge University Press

2. Preliminaries

2.1. Existence, uniqueness, and boundedness of solutions

Let $\mathbf{C} = C([-\tau, 0], \mathbb{R}_+)$ be a set of continuous functions mapping $[-\tau, 0]$ to $\mathbb{R}_+$ equipped with the supremum norm, where $\mathbb{R}_+$ is the set of positive real numbers. Consider the initial data $\phi = (\phi_1(t), \phi_2(t)) \in \mathbf{C} \times \mathbf{C}$ for system (1.2). The right-hand side of system (1.2) is continuously differentiable with respect to the arguments $x(t)$, $y(t)$, $x(t-\tau)$, and $y(t-\tau)$. By the existence and uniqueness theorem [8, 14], there exists a unique solution $(x_1(t), x_2(t))$ for t in a small neighbourhood of $t = 0$ and satisfies the initial condition $(x_1(t), x_2(t)) = (\phi_1(t), \phi_2(t))$ for $t \in [-\tau, 0]$. Moreover, the solution is continuously differentiable.

Lemma 2.1. *$x(t)$ and $y(t)$ are positive for $t > 0$ given the initial condition $\phi \in \mathbf{C} \times \mathbf{C}$.*

Proof. It follows from the first equation of system (1.2) and the formula of variation of constants that

$$x(t) = x(0)e^{\int_0^t r(1-\frac{x(s)}{K}) - \frac{my(s)}{a+x(s)}\,ds}.$$

Since $x(0) > 0$, then $x(t) > 0$ for $t > 0$ on the interval of existence. For $y(t)$, since $y(0) > 0$ and $y(t)$ is continuous, then either $y(t) > 0$ for $t > 0$ on the interval of existence, or $\exists\ t_0 > 0$, such that $y(t_0) = 0$, but $y'(t_0) \le 0$. However, by substituting $t = t_0$ into the second equation of system (1.2), we obtain

$$y'(t_0) = e^{-d\tau}\frac{cmx(t_0-\tau)y(t_0-\tau)}{a + x(t_0-\tau)} > 0,$$

Which is a contradiction. Hence, $y(t)$ is positive for $t > 0$. □

Lemma 2.2. *The solution $(x(t), y(t))$ is eventually uniformly bounded from above provided that the initial condition $\phi \in \mathbf{C} \times \mathbf{C}$.*

Proof. We will first show that $x(t)$ is eventually uniformly bounded from above. From the first equation of system (1.2), by Lemma 2.1, we have

$$\frac{dx}{dt} = rx(t)\left(1 - \frac{x(t)}{K}\right) - \frac{mx(t)y(t)}{a + x(t)} < rx(t)\left(1 - \frac{x(t)}{K}\right).$$

Let $X(t)$ be the solution to $\frac{dX}{dt} = X(t)(1 - \frac{X(t)}{K})$ with $X(0) = x(0) > 0$. By the comparison theorem,

$$\limsup_{t\to\infty} x(t) \le \limsup_{t\to\infty} X(t) = K.$$

To show $y(t)$ is eventually uniformly bounded from above, let $U(t) = ce^{-d\tau}x(t-\tau) + y(t)$, then

$$\begin{aligned}\frac{dU}{dt} &= ce^{-d\tau}\frac{d(x(t-\tau))}{dt} + \frac{d(y(t))}{dt}\\ &= ce^{-d\tau}\left((r+d)x(t-\tau) - \frac{r(x(t-\tau))^2}{K}\right) - dU(t).\end{aligned}$$

Notice that

$$(r+d)x(t-\tau) - \frac{r(x(t-\tau))^2}{K} - \frac{(r+d)^2K}{4r} = -\left(\frac{\sqrt{r}x(t-\tau)}{\sqrt{K}} - \frac{(r+d)\sqrt{K}}{2\sqrt{r}}\right)^2 \le 0,$$

and accordingly,

$$\frac{dU}{dt} \le ce^{-d\tau}\frac{(r+d)^2K}{4r} - dU(t).$$

Let $Y(t)$ be the solution to $\frac{dY}{dt} = ce^{-d\tau}\frac{(r+d)^2K}{4r} - dY(t)$ with $Y(0) = U(0)$. Then,

$$Y(t) = \frac{ce^{-d\tau}(r+d)^2K}{4rd} + \left(U(0) - \frac{ce^{-d\tau}(r+d)^2K}{4rd}\right)e^{-dt}.$$

https://doi.org/10.1017/S0956792526100370 Published online by Cambridge University Press

By the comparison theorem,

$$\limsup_{t\to\infty} y(t) \le \limsup_{t\to\infty} U(t) \le \limsup_{t\to\infty} Y(t) = \frac{ce^{-d\tau}(r+d)^2K}{4rd} \le cK.$$

Hence, $y(t)$ is eventually uniformly bounded from above. □

Theorem 2.3. *The solution $(x(t), y(t))$ of system (1.2) exists on $[-\tau, \infty)$ for $\phi \in \mathbf{C} \times \mathbf{C}$.*

Proof. By Lemmas 2.1 and 2.2, the solution $(x(t), y(t))$ is eventually uniformly bounded. By the Continuation Theorem [8, 14], the solution exists for all $t > 0$. □

2.2. Dynamics of the classical model and equilibrium points of system (1.2)

To fully understand the dynamics of the delayed model (1.2), we recall the dynamics of the classical model below, i.e., the corresponding ODE system of model (1.2), which was studied by Jing and Chen in the 1980s [13].

$$\begin{cases} \dfrac{dx(t)}{dt} = rx\left(1 - \dfrac{x}{K}\right) - \dfrac{mxy}{a+x}, \\ \dfrac{dy(t)}{dt} = y\left(-d + \dfrac{cmx}{a+x}\right). \end{cases} \tag{2.1}$$

Lemma 2.4. *Let $K_c = \frac{ad}{cm-d}$, and $K_0 = \frac{a(cm+d)}{cm-d}$. System (2.1) has three equilibrium points $E_0(0,0)$, $E_K(K,0)$ and $E^*(\frac{ad}{cm-d}, \frac{rca(Kcm-Kd-ad)}{K(cm-d)^2})$, where E_0 is always a saddle.*

- *E_K is globally asymptotically stable for $K < K_c$ and becomes unstable for $K > K_c$. As K increases and crosses the threshold $K = K_c$, a transcritical bifurcation takes place between E_K and E^*. E_K loses stability and E^* enters the first quadrant.*
- *$K = K_0$ is the Hopf bifurcation threshold for E^*. E^* is globally asymptotically stable for $K_c < K < K_0$ and unstable for $K > K_0$.*
- *System (2.1) has no periodic solution for $K \le K_0$, and a unique periodic solution for $K > K_0$.*

For system (1.2), it is easy to see that the equilibrium points $E_0(0,0)$ and $E_K(K,0)$ exist for all $\tau > 0$. To explore the existence and stability of interior equilibrium points, we define the following parameters for convenience:

$$K_1 = \frac{ad}{cme^{-d\tau} - d}, K_2 = \frac{ad(3cm+d)}{c^2m^2 - d^2}, \tau_{max} = \frac{1}{d}\ln\left(\frac{Kcm}{ad+dK}\right).$$

Then, $K_c < K_2 < K_0$ and $K_c < K_1$. We introduce the condition below.

- Condition C_0 : $cm > d$, and $K > K_1$ (i.e., $\tau < \tau_{max}$).

Through straightforward calculations, we derive the following lemma.

Lemma 2.5. *The interior equilibrium $E^*(\frac{da}{ce^{-d\tau}m-d}, \frac{rce^{-d\tau}a(Kce^{-d\tau}m-Kd-da)}{K(ce^{-d\tau}m-d)^2})$ of system (1.2) exists under the condition C_0.*

Consider the stability of equilibrium points. Let (x_0, y_0) be any equilibrium point of system (1.2) The characteristic matrix at (x_0, y_0) is given by

$$J(x_0,y_0) = \begin{bmatrix} \left(r - \frac{2rx_0}{K} - \frac{may_0}{(a+x_0)^2}\right) - \lambda & \frac{-mx_0}{a+x_0} \\ e^{-\lambda\tau}\frac{ce^{-d\tau}may_0}{(a+x_0)^2} & \left(-d + e^{-\lambda\tau}\frac{ce^{-d\tau}mx_0}{(a+x_0))}\right) - \lambda \end{bmatrix}.$$

https://doi.org/10.1017/S0956792526100370 Published online by Cambridge University Press

By substituting x_0 and y_0 with 0 in $J(x_0, y_0)$, we obtain two simple eigenvalues of $J(0,0)$: $\lambda_1 = r > 0$ and $\lambda_2 = -d < 0$. Applying the Hartman–Grobman theorem [9], we establish the following lemma.

Lemma 2.6. *Equilibrium E_0 is a saddle point for all $\tau \geq 0$.*

3. Local dynamics near equilibrium points

3.1. Local stability of E^*

Substituting the coordinates of E^* into $J(x_0, y_0)$, we obtain

$$J(E^*) = \begin{bmatrix} \frac{rd(K(ce^{-d\tau}m-d)-a(ce^{-d\tau}m+d))}{Kce^{-d\tau}m(ce^{-d\tau}m-d)} - \lambda & \frac{-d}{ce^{-d\tau}} \\ e^{-\lambda\tau}\frac{r(Kce^{-d\tau}m-Kd-da)}{Km} & -d + de^{-\lambda\tau} - \lambda \end{bmatrix}.$$

The characteristic equation is derived by setting the determinant of $J(E^*)$ to zero, i.e.,

$$P(\lambda, \tau) := \lambda^2 + [d - H(\tau)]\lambda + e^{-\lambda\tau}[-d\lambda + L(\tau)] - dH(\tau) = 0, \tag{3.1}$$

where $H(\tau)$ and $L(\tau)$ are defined as follows

$$H(\tau) = r\left[\frac{de^{d\tau}}{cm} - \frac{ad}{K(ce^{-d\tau}m - d)} - \frac{ad^2e^{d\tau}}{(ce^{-d\tau}m - d)Kcm}\right],$$

$$L(\tau) = dH(\tau) + A(\tau), \text{ and } A(\tau) = rd\left(\frac{Kce^{-d\tau}m - Kd - da}{Kmce^{-d\tau}}\right),$$

with $\tau \in [0, \tau_{max})$. Under condition C_0, $A(\tau)$ is strictly positive, and the functions $H(\tau)$, $L(\tau)$, and $A(\tau)$ are well defined and bounded. For simplicity, we will drop the (τ) and express $H(\tau)$, $L(\tau)$, and $A(\tau)$ as H, L, and A when necessary.

Lemma 3.1. *The sum of the multiplicity of roots of $P(\lambda, \tau) = 0$ on $\mathbb{C}^+ = \{\lambda \in \mathbb{C} : Re(\lambda) > 0\}$ can change only if a pair of conjugate complex roots appear on or cross the imaginary axis as τ varies continuously on $[0, \tau_{max})$.*

Proof. To show that no eigenvalue emerges from infinity, we write $P(\lambda, \tau) = \lambda^2 + \eta(\lambda, \tau)$, where $\eta(\lambda, \tau) = [d - H(\tau)]\lambda + e^{-\lambda\tau}[-d\lambda + L(\tau)] - dH(\tau)$. Since $H(\tau)$ and $L(\tau)$ are bounded on $[0, \tau_{max})$, we have

$$\limsup_{Re\lambda>0, |\lambda|\to\infty} \left|\lambda^{-2}\eta(\lambda, \tau)\right| \leq \limsup_{Re\lambda>0, |\lambda|\to\infty} \left(\frac{2d + |H(\tau)|}{|\lambda|} + \frac{|L(\tau)| + d|H(\tau)|}{|\lambda|^2}\right) = 0 < 1.$$

Furthermore, $P(0, \tau) = A(\tau) > 0$ for $\tau \in [0, \tau_{max})$. Hence, $\lambda = 0$ is not a root for $\tau \in [0, \tau_{max})$. By Theorem 1.4, Chapter 3 of [14], the desired result is obtained. □

To study the stability of E^* and the possibility of Hopf bifurcation at E^* as τ varies, by Lemma 3.1, we assume $\lambda = \pm iw$ is a pair of purely imaginary roots of $P(\lambda, \tau) = 0$ where $w > 0$. This leads to

$$-w^2 + [d - H]iw + e^{-i\tau w}[-diw + L] - dH = 0.$$

Using Euler's formula and equating the real and imaginary parts to zero, we obtain

$$\begin{cases} -w^2 + L\cos(\tau w) - dw\sin(\tau w) - dH = 0, \\ (d - H)w - dw\cos(\tau w) - L\sin(\tau w) = 0. \end{cases} \tag{3.2}$$

https://doi.org/10.1017/S0956792526100370 Published online by Cambridge University Press

Solving for $\cos(\tau w)$ and $\sin(\tau w)$, and using the assumption $\tau \in [0, \tau_{max})$, we obtain

$$\begin{cases} \sin(\tau w) = \frac{dwL - HwL - d^2wH - dw^3}{L^2 + d^2w^2}, \\ \cos(\tau w) = \frac{LdH + Lw^2 + (dw)^2 - dHw^2}{L^2 + d^2w^2}. \end{cases} \tag{3.3}$$

Both $\sin(\tau w)$ and $\cos(\tau w)$ are well defined, since $L^2 \geq 0$ and $d^2w^2 > 0$. Applying $\sin^2(\tau w) + \cos^2(\tau w) = 1$ to (3.3), we obtain

$$(d^2w^2 + L^2)(w^4 + H^2w^2 + d^2H^2 - L^2) = 0. \tag{3.4}$$

Theorem 3.2. *Let $K > K_2$, and define*

$$\bar{\tau} = \frac{1}{d} \ln \left(\frac{cm\sqrt{9a^2 + 4aK + 4K^2} - 3acm}{2(ad + dK)} \right).$$

The following statements hold.

(1) $0 < \bar{\tau} < \tau_{max}$.

(2) $L(\tau) + dH(\tau) > 0$ *if* $\tau \in [0, \bar{\tau})$, $L(\tau) + dH(\tau) = 0$ *if* $\tau = \bar{\tau}$, *and* $L(\tau) + dH(\tau) < 0$ *if* $\tau \in (\bar{\tau}, \tau_{max})$.

(3) *The unique solution of the hexic equation (3.4) for* $0 \leq \tau < \bar{\tau}$ *and* $K > K_2$ *is given by*

$$w(\tau) = \sqrt{\frac{\sqrt{((H(\tau))^4 - 4d^2(H(\tau))^2 + 4(L(\tau))^2)}}{2} - \frac{(H(\tau))^2}{2}}. \tag{3.5}$$

Proof. Statement (1) is obtained by direct calculation.

(2). $L(\tau) + dH(\tau)$ is continuous for $\tau \in [0, \tau_{max})$. It is easy to check that $L(\tau) + dH(\tau)$ equals zero if and only if $\tau = \bar{\tau}$, and

$$L'(\bar{\tau}) + dH'(\bar{\tau}) = -\frac{4ard^2(K + a)(\sqrt{4K^2 + 4Ka + 9a^2} - 3a)}{(2K + 5a - \sqrt{4K^2 + 4Ka + 9a^2})^2 K} < 0.$$

Hence, the sign of $L(\tau) + dH(\tau)$ is obtained for $\tau \in [0, \tau_{max})$.

(3) Let $Z = w^2$, and substitute Z into the hexic equation (3.4). Then, three solutions appear

$$Z_{\pm} = \frac{\pm\sqrt{H^4 - 4d^2H^2 + 4L^2}}{2} - \frac{H^2}{2}, Z_3 = \frac{-L^2}{d^2}.$$

Since $Z = w^2 > 0$, Z_- and Z_3 are discarded. To ensure $w = \sqrt{Z_+}$ is well defined, it suffices to show

$$(H(\tau))^4 - 4d^2(H(\tau))^2 + 4(L(\tau))^2 > (H(\tau))^4,$$

i.e., $(L(\tau))^2 > d^2(H(\tau))^2$. Since $A(\tau)$ is positive for $\tau \in [0, \tau_{max})$, we have $L(\tau) = dH(\tau) + A(\tau) > dH(\tau)$. Moreover, by statement (2), we have $L(\tau) > -dH(\tau)$ for $\tau \in [0, \bar{\tau})$. In conclusion, $L(\tau) > |dH(\tau)|$, and $(L(\tau))^2 > d^2(H(\tau))^2$. □

Corollary 3.3. *The equilibrium E^* is locally asymptotically stable if $K \leq K_2$ and $\tau \in (0, \tau_{max})$, or $K_2 < K < K_0$ and $\tau \in [\bar{\tau}, \tau_{max})$.*

Proof. Based on Theorem 3.2, $d^2(H(\tau))^2 - (L(\tau))^2 > 0$ if $K \leq K_2$ and $\tau \in (0, \tau_{max})$, or $K_2 < K < K_0$ and $\tau \in [\bar{\tau}, \tau_{max})$. Then, (3.4) has no positive root and the desired result follows. □

3.2. Local Hopf bifurcation at E^*

By statement (3) of Theorem 3.2, we assume $0 \leq \tau \leq \bar{\tau} < \tau_{max}$ and $K > K_2$, which guarantees that the hexic equation (3.4) has a positive root $w = w(\tau)$, a necessary condition for Hopf bifurcation.

https://doi.org/10.1017/S0956792526100370 Published online by Cambridge University Press

We explore the critical values for $\tau \in [0, \bar{\tau})$ at which Hopf bifurcation occurs. From the second equation of system (3.3), it is reasonable to define the angle $\tau w(\tau)$ using the inverse cosine function, while also considering the sign of $\sin(\tau w(\tau))$. Here $\sin(\tau w(\tau))$ is the composition of the functions $\sin(\tau w)$ and $w(\tau)$, which are given by the first equation of system (3.3) and equation (3.5), respectively.

Lemma 3.4. *Define* $\check{\tau} = \frac{1}{d} \ln\left(\frac{cm(K-a)}{d(K+a)}\right)$.

(1) *If* $K < K_0$, *then* $\check{\tau} < 0$, *or* $\check{\tau}$ *does not exist, and* $\sin(\tau w(\tau)) > 0$ *for all* $\tau \in [0, \bar{\tau})$.

(2) *If* $K = K_0$, *then* $\check{\tau} = 0$, $\sin(\check{\tau} w(\check{\tau})) = 0$. *Moreover,* $\sin(\tau w(\tau)) > 0$ *for all* $\tau \in (0, \bar{\tau})$.

(3) *If* $K > K_0$, $\check{\tau}$ *is well defined with* $0 < \check{\tau} < \bar{\tau}$. *Then,* $\sin(\tau w(\tau))$ *changes sign as follows:* $\sin(\tau w(\tau)) < 0$ *for* $0 < \tau < \check{\tau}$; $\sin(\tau w(\tau)) = 0$ *for* $\tau = \check{\tau}$; $\sin(\tau w(\tau)) > 0$ *for* $\check{\tau} < \tau < \bar{\tau}$.

Consequently, the function $\theta_n(\tau)$, $\tau \in [0, \bar{\tau})$ *is well defined as follows.*

- *If* $\sin(\tau w(\tau)) < 0$: $\theta_n(\tau) = -\arccos\left(\frac{LdH + Lw^2 + d^2w^2 - dHw^2}{L^2 + d^2w^2}\right) + 2n\pi$.
- *If* $\sin(\tau w(\tau)) \geq 0$: $\theta_n(\tau) = \arccos\left(\frac{LdH + Lw^2 + d^2w^2 - dHw^2}{L^2 + d^2w^2}\right) + 2n\pi$.

Here, $n \in \mathbb{N}$, *and* $\mathbb{N}$ *is the set of all nonnegative integers.*

Proof. Solving $\sin(\tau w(\tau)) = 0$ for $H(\tau)$, we obtain three solutions

$$H(\tau) = 0, H(\tau) = \frac{L(\tau)}{d}, H(\tau) = 2d.$$

The solution $H(\tau) = \frac{L(\tau)}{d}$ is discarded since it is valid only for $\tau = \tau_{max}$. The third solution $H(\tau) = 2d$ is also discarded. Indeed, substituting $H(\tau) = 2d$ into $\sin(\tau w(\tau)) = 0$ yields $|L(\tau)| + L(\tau) = 0$. Since $A(\tau) > 0$, we have

$$0 < 2d^2 + A(\tau) = dH(\tau) + A(\tau) = L(\tau) = -|L(\tau)| \leq 0,$$

which leads to a contradiction. Therefore, the remaining solution $H(\tau) = 0$ holds when $\tau = \check{\tau}$.

Case (1). If $K < K_0$, then $\check{\tau} < 0$, or $\check{\tau}$ does not exist. Then, $H(\tau) < 0$ for all $\tau \in [0, \bar{\tau})$. By continuity, $\sin(\tau w(\tau))$ does not change sign as τ varies in $[0, \bar{\tau})$. We are now investigating the sign of $\sin(\tau w(\tau))$.

Since $L(\tau) = dH(\tau) + A(\tau)$ and $w(\tau)$ is given by (3.5), we obtain

$$\operatorname{sign}\{\sin(\tau w(\tau)\} = \operatorname{sign}\{dL(\tau) - H(\tau)L(\tau) - d^2H(\tau) - d(w(\tau))^2\} = \operatorname{sign}\{\xi_1 - \xi_2\},$$

where $\xi_1 = 2dA(\tau) - d(H(\tau))^2 - 2A(\tau)H(\tau)$ and $\xi_2 = d\sqrt{(H(\tau))^4 + 8dA(\tau)H(\tau) + 4(A(\tau))^2}$.

Since $L(\tau) > -dH(\tau)$ for $\tau \in [0, \bar{\tau})$, it follows that $A(\tau) = L(\tau) - dH(\tau) > -2dH(\tau)$. Noting that $H(\tau) < 0$, we get $\xi_1 > 3d(H(\tau))^2 - 4d^2H(\tau) = dH(\tau)(3H(\tau) - 4d) > 0$. It is apparent that $\xi_2 \geq 0$.

Next, we analyse the sign of $\xi_1^2 - \xi_2^2$. Since $H(\tau) < 0$, we obtain

$$\begin{aligned}\operatorname{sign}\{\xi_1^2 - \xi_2^2\} &= \operatorname{sign}\{A(\tau)H(\tau)\,(H(\tau) - 2d)\,\left(dH(\tau) + A(\tau) + d^2\right)\} \\ &= \operatorname{sign}\{dH(\tau) + A(\tau) + d^2\} > 0.\end{aligned}$$

Since $A(\tau) > -2dH(\tau)$, it follows that $dH(\tau) + A(\tau) + d^2 > -dH(\tau) + d^2 > 0$. Thus, $\xi_1^2 - \xi_2^2 > 0$, implying $\xi_1 > \xi_2 > 0$. Hence,

$$\operatorname{sign}\{\sin(\tau w(\tau)\} = \operatorname{sign}\{\xi_1 - \xi_2\} = \frac{\operatorname{sign}\{\xi_1^2 - \xi_2^2\}}{\operatorname{sign}\{\xi_1 + \xi_2\}} = 1,\ \forall \tau \in [0, \bar{\tau}).$$

Cases (2) and (3). Since $K_0 > a$, if $K \geq K_0$, then $\check{\tau}$ is well defined. In this case, to study the sign of $\sin(\tau w(\tau))$, it suffices to check the sign of its derivative at $\check{\tau}$. We have

$$\frac{d}{d\tau}(\sin(\tau w(\tau)))\Big|_{\tau=\check{\tau}} = \frac{\sqrt{\frac{ard}{K}}\ (a-K)^2}{2a^2} > 0,$$

and which implies that $\sin(\tau w(\tau))$ changes sign from negative to positive at $\check{\tau}$. The additional condition $K > K_0$ ensures that $\check{\tau}$ is positive, and the desired results follow. □

https://doi.org/10.1017/S0956792526100370 Published online by Cambridge University Press

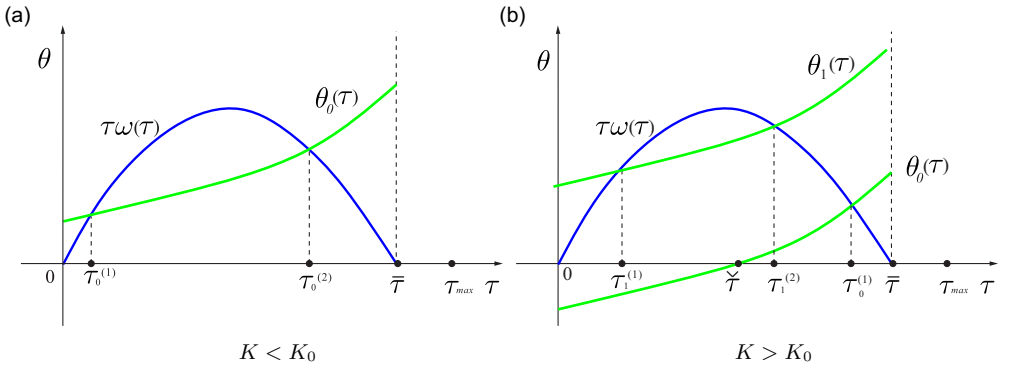


Figure 1. *Intersection of $\tau w(\tau)$ and $\theta_n(\tau)$. Here, the graphs of $\tau w(\tau)$ and $\theta_n(\tau)$ are sketched in a relatively simple way, but ensuring that the properties of Lemma 3.5 are all satisfied.*

By Theorem 3.2 and Lemma 3.4, we obtain two functions

$$\theta = \tau w(\tau),\ \theta = \theta_n(\tau), \tau \in [0, \bar{\tau}].$$

See Figure 1. These two functions are defined at $\tau = \bar{\tau}$ by continuous extension. The following lemma is obvious.

Lemma 3.5. *Consider two functions $\theta = \tau w(\tau)$ and $\theta = \theta_n(\tau)$, where $n \in \mathbb{N}$.*

(1) *$\theta = \tau w(\tau) \geq 0$ on $\tau \in [0, \bar{\tau}]$ and vanishes only at $\tau = 0$ and $\tau = \bar{\tau}$.*

(2) *$\theta_0(0) > 0 (= 0, < 0$, resp.$)$ if $K < K_0 (= K_0, > K_0$, resp$)$.*

(3) *$\theta_0(\bar{\tau}) = \pi$ regardless of K.*

(4) *If $K < K_0$, then there exists $\zeta > 0$ such that $0 < \zeta \leq \theta_0(\tau) \leq \pi$ for $\tau \in [0, \bar{\tau}]$.*

Proof. Statements (1) and (2) follow from Theorem 3.2 and Lemma 3.4.

For statements (3) and (4), a straightforward calculation gives $\sin(\bar{\tau} w(\bar{\tau})) = 0$ and $\cos(\bar{\tau} w(\bar{\tau})) = -1$, which implies that $\theta_0(\bar{\tau}) = \pi$. Since $\theta_0(\tau)$ is continuous on $[0, \bar{\tau}]$, it attains the maximum and minimum values on $[0, \bar{\tau}]$. By statement (1) of Lemma 3.4, $\sin(\tau w(\tau)) > 0$ for all $\tau \in [0, \bar{\tau})$, so $\zeta = \min_{\tau \in [0, \bar{\tau}]} \theta_0(\tau) > 0$ and $\max_{\tau \in [0, \bar{\tau}]} \theta_0(\tau) = \pi$. □

Theorem 3.6. *Assume that there exists $\tau^\star \in (0, \bar{\tau})$ such that*

$$\tau w(\tau)_{|\tau^\star} = \theta_n(\tau)_{|\tau^\star},\ \text{and}\ (\tau w(\tau))'_{|\tau^\star} \neq (\theta_n(\tau))'_{|\tau^\star}$$

for some $n \in \mathbb{N}$. Then system (1.2) undergoes a Hopf bifurcation at $\tau = \tau^\star$, and a family of non-constant periodic solutions exists in a neighbourhood of E^* for τ in a small neighbourhood of $\tau = \tau^\star$.

Proof. Let $\lambda(\tau) = \alpha(\tau) \pm i\beta(\tau)$ be a pair of conjugate complex eigenvalues of $P(\lambda, \tau) = 0$. The condition $\tau w(\tau)_{|\tau^\star} = \theta_n(\tau)_{|\tau^\star}$ implies that $\alpha(\tau^\star) = 0$ and $\beta(\tau^\star) = w(\tau^\star) > 0$, meaning that $P(\lambda, \tau) = 0$ has a pair of purely imaginary eigenvalues $\pm i w(\tau^\star)$ at $\tau = \tau^\star$. Next, we check the transversality condition by defining the function

$$S_n(\tau) = \tau - \frac{\theta_n(\tau)}{w(\tau)}, n \in \mathbb{N}.$$

By Theorem 2.2 of [3] (the geometric stability switch criterion), we obtain

$$\delta(\tau^\star) := \operatorname{sign}\left\{\frac{d\alpha(\tau)}{d\tau}\bigg|_{\tau=\tau^\star}\right\} = \operatorname{sign}\left\{\frac{dF(w(\tau))}{dw}\bigg|_{\tau=\tau^\star}\right\} \cdot \operatorname{sign}\left\{\frac{dS_n(\tau)}{d\tau}\bigg|_{\tau=\tau^\star}\right\},$$

where $F(w(t)) = (w(\tau))^4 + (H(\tau))^2(w(\tau))^2 + d^2(H(\tau))^2 - (L(\tau))^2$. Thus,

$$F_w(w(\tau)) = 4(w(\tau))^3 + 2(H(\tau))^2 w(\tau) > 0,\ \forall \tau \in (0, \bar{\tau}).$$

https://doi.org/10.1017/S0956792526100370 Published online by Cambridge University Press

By the definition of $S_n(\tau)$, we have

$$\frac{dS_n(\tau)}{d\tau} = 1 - \frac{\theta_n'(\tau)w(\tau) - w'(\tau)\theta_n(\tau)}{(w(\tau))^2} = \frac{\tau(w(\tau))^2 - [\theta_n'(\tau)\tau w(\tau) - \tau w'(\tau)\theta_n(\tau)]}{\tau(w(\tau))^2}.$$

Since $(\tau w(\tau))' = \tau w'(\tau) + w(\tau)$, we get $\tau w'(\tau) = (\tau w(\tau))' - w(\tau)$. Noting that $\theta_n(\tau^\star) = \tau^\star w(\tau^\star)$, we obtain

$$\begin{aligned}\left.\frac{dS_n(\tau)}{d\tau}\right|_{\tau=\tau^\star} &= \frac{\tau^\star(w(\tau^\star))^2 - \theta_n'(\tau^\star)\tau^\star w(\tau^\star) + \left[(\tau w(\tau))'_{|\tau^\star} - w(\tau^\star)\right]\tau^\star w(\tau^\star)}{\tau^\star(w(\tau^\star))^2} \\ &= \frac{\tau^\star w(\tau^\star)\left[(\tau w(\tau))'_{|\tau^\star} - \theta_n'(\tau^\star)\right]}{\tau^\star(w(\tau^\star))^2} = \frac{(\tau w(\tau))'_{|\tau^\star} - \theta_n'(\tau^\star)}{w(\tau^\star)}.\end{aligned}$$

Since $w(\tau^\star) > 0$, we obtain

$$\delta(\tau^\star) = \operatorname{sign}\{(\tau w)' - \theta_n'(\tau)_{|\tau=\tau^\star}\} \neq 0,$$

which completes the proof. □

Remark 3.7. *$\delta(\tau^\star)$ reveals the direction along which the complex conjugate eigenvalues $\lambda = \alpha(\tau) \pm i\beta(\tau)$ cross the imaginary axis as τ increases through $\tau = \tau^\star$. If $\delta(\tau^\star) = 1$ (resp. $\delta(\tau^\star) = -1$), λ crosses the imaginary axis from left to right (resp. from right to left). If $\delta(\tau^\star) \neq 0$, the graphs of two functions $\theta = \tau w(\tau)$ and $\theta = \theta_n(\tau)$ intersect transversely at $\tau = \tau^\star$. Otherwise, the two graphs are tangent.*

It is technically challenging to characterize the number of intersections between $\theta = \tau w(\tau)$ and $\theta = \theta_n(\tau)$ or the roots of $S_n(\tau) = 0$, $n \in \mathbb{N}$. There may be no roots or several roots.

Definition 3.8. *Let $\chi(n)$ be the number of roots of $S_n(\tau) = 0$ on $(0, \bar{\tau})$, where $n \in \mathbb{N}$.*

The following hypothesis is necessary for the occurrence of Hopf bifurcation.

(H1) Suppose that $S_n(\tau) = 0$ has finitely many roots on $(0, \bar{\tau})$, i.e., $0 \leq \chi(n) < \infty, \forall n \in \mathbb{N}$, and these $\chi(n)$ roots are given and arranged in the following order

$$\tau_n^{(1)} < \tau_n^{(2)} < \cdots < \tau_n^{(i)} < \cdots \tau_n^{(\chi(n))},$$

with $\delta(\tau_n^{(i)}) = \pm 1$ $(i = 1, 2, \cdots, \chi(n))$.

Remark 3.9. *Let $\Lambda = \{j \in \mathbb{N} | \chi(j) \neq 0\}$. If $\chi(n) = 2$ for all $n \in \Lambda$, then we denote $\tau_n^{(1)}$ and $\tau_n^{(2)}$ as τ_n^- and τ_n^+, respectively.*

Example 1. *Two sets of parameters are chosen to show the distribution of roots of $S_n(\tau) = 0$.*

(a) *Choose $K = 1, r = 30, m = 1, c = 4, d = 0.1, a = 1$. See Figure 2(a). Here, $K < K_0 = \frac{41}{39}$, and we have $\chi(0) = \chi(1) = \chi(2) = \chi(3) = 2$, and $\chi(n) = 0$ for $n \geq 4$. The critical Hopf bifurcation values are*

$$\begin{aligned}&\tau_0^- = 0.013562,\ \tau_0^+ = 23.67336,\ \tau_1^- = 3.8062,\quad \tau_1^+ = 21.49988,\\ &\tau_2^- = 7.81234,\quad \tau_2^+ = 19.55209,\ \tau_3^- = 12.7067,\ \tau_3^+ = 17.10348.\end{aligned}$$

(b) *Choose $K = 20, r = 10, m = 1, c = 4, d = 0.1, a = 5$. See Figure 2(b). Here, $K > K_0 = \frac{205}{39}$, and we have $\chi(0) = 1$, $\chi(1) = 2$, $\chi(2) = 4$, and $\chi(n) = 0$ for $n \geq 3$. The critical Hopf bifurcation values are*

$$\begin{aligned}&\tau_0^{(1)} = 32.42808,\ \tau_1^{(1)} = 6.2049,\quad \tau_1^{(2)} = 32.22374,\\ &\tau_2^{(1)} = 13.96008,\ \tau_2^{(2)} = 24.85518,\ \tau_2^{(3)} = 30.21286,\ \tau_2^{(4)} = 32.00694.\end{aligned}$$

Corollary 3.10. *Assume (H1), then Hopf bifurcation occurs at a sequence of critical values $\tau = \tau_n^{(i)}$ and there exists a family of non-constant periodic solutions in a neighbourhood of E^* for τ in a small neighbourhood of $\tau = \tau_n^{(i)}$.*

https://doi.org/10.1017/S0956792526100370 Published online by Cambridge University Press

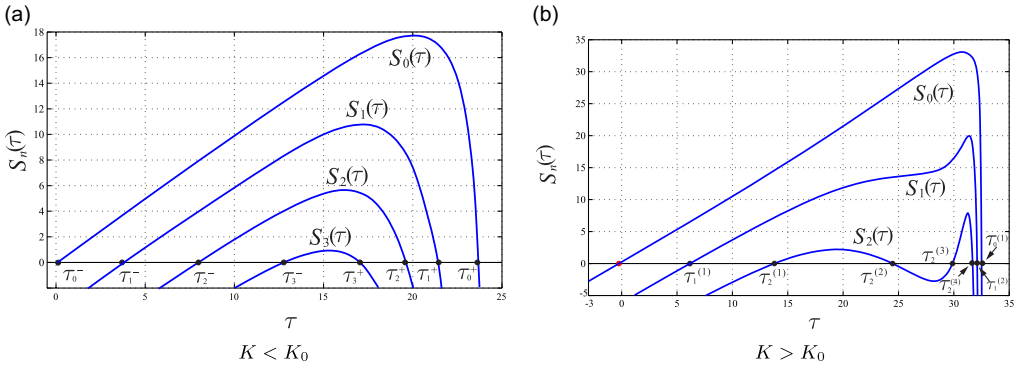


Figure 2. *Left panel: Roots of $S_n(\tau) = 0$ for the parameters given in Example 1(a), where $K < K_0$. Right panel: Roots of $S_n(\tau) = 0$ for the parameters given in Example 1(b), where $K > K_0$.*

The following is an attempt to study the roots of $S_n(\tau) = 0$ for certain special cases.

Proposition 3.11. *Let $M = \max_{\tau\in[0,\bar{\tau}]}\{\tau w(\tau)\}$. Assume that*

$$K < K_0, \text{ and } (2N+1)\pi < M < (2N+3)\pi$$

for some $N \in \mathbb{N}$. Then, there are three cases.

(1) *If $n \le N$, $\theta_n(\tau)$ intersects $\tau w(\tau)$ at least twice.*

(2) *If $n = N+1$, $\theta_n(\tau)$ and $\tau w(\tau)$ intersect either at least twice, or once tangentially, or they never intersect.*

(3) *If $n \ge N+2$, $\theta_n(\tau)$ and $\tau w(\tau)$ never intersect in $(0, \bar{\tau})$.*

Proof. By Lemma 3.5, $\theta_n(\tau)$ ranges between $[\zeta + 2n\pi, (2n+1)\pi]$. From statement (1) of Lemma 3.5, we have $\tau w(\tau)\big|_{\tau=0} = 0$ and $\tau w(\tau)\big|_{\tau=\bar{\tau}} = 0$ and $M > 0$. For the first case, from the intermediate value theorem, it follows that $\theta_n(\tau)$ must intersect $\tau w(\tau)$ at least twice since $\theta_n(0) \ge \zeta + 2n\pi > 0$, $M > (2N+1)\pi > \max_{\tau\in[0,\bar{\tau}]}\theta_n(\tau)$, and $\theta_n(\bar{\tau}) > 0$. For the third case, we have $n \ge N+2$, hence $\min_{\tau\in[0,\bar{\tau}]}\theta_n(\tau) > 2n\pi \ge 2(N+2)\pi > M$ and the result follows. The second case is trivial, as all possibilities might hold here. □

3.3. Local dynamics and bifurcations involving E_K

Theorem 3.12.

(1) E_K is asymptotically stable for $\tau > \tau_{max}$ and unstable for $0 < \tau < \tau_{max}$.

(2) System (1.2) undergoes a transcritical bifurcation involving E_K and E^* at $\tau = \tau_{max}$.

Proof. (1) The characteristics equation at E_K has the following form

$$(\lambda + r)\left(\lambda + d - \frac{ce^{-d\tau}mK}{a+K}e^{-\lambda\tau}\right) = 0.$$

Therefore, $\lambda = -r$ is an eigenvalue, and the other eigenvalues are the roots of the equation

$$Q(\lambda) := \lambda + d - \frac{ce^{-d\tau}mK}{a+K}e^{-\lambda\tau} = 0. \tag{3.6}$$

As one did for E^*, an analogous analysis can be performed to investigate the stability of E_K. Here, using Theorem 4.7(a) in Chapter 4 of [22] we conclude that E_K is asymptotically stable if $\tau > \tau_{max}$. If

https://doi.org/10.1017/S0956792526100370 Published online by Cambridge University Press

$0 < \tau < \tau_{max}$, then $Q(0) < 0$. Note that $\lim_{\lambda\to\infty,\lambda\in\mathbb{R}} Q(\lambda) = \infty$, by continuity of $Q(\lambda)$, there exists a positive real root. Hence, E_K is always unstable.

(2) If $\tau = \tau_{max}$, then $E_K = E^*$ and $Q(0) = 0, Q'(0) = 1 + d\tau_{max} \neq 0$. Hence, $\lambda = 0$ is a simple eigenvalue.

Let $\hat{\lambda}(\tau)$ be a root of $Q(\lambda) = 0$ such that $\hat{\lambda}(\tau_{max}) = 0$. To verify that E_K changes stability at $\tau = \tau_{max}$, we compute

$$\frac{d}{d\tau}\mathrm{Re}(\hat{\lambda})\Big|_{\tau=\tau_{max}} = -\frac{cmdKe^{-d\tau}}{a+K+\tau cmKe^{-d\tau}}\Big|_{\tau=\tau_{max}} < 0.$$

As a consequence, E_K changes stability from unstable to stable. To investigate the stability switch of E^* at $\tau = \tau_{max}$, let $\tilde{\lambda}(\tau)$ be a root of $P(\lambda, \tau) = 0$ such that $\tilde{\lambda}(\tau_{max}) = 0$. By the chain rule, we have

$$\frac{dP(\lambda,\tau)}{d\tau} = \frac{\partial P(\lambda,\tau)}{\partial\lambda}\frac{d\lambda}{d\tau} + \frac{\partial P(\lambda,\tau)}{\partial\tau} = 0.$$

Substituting $\tau = \tau_{\max}$ and using $\tilde{\lambda}(\tau_{\max}) = 0$, we obtain

$$\frac{dP(\lambda,\tau)}{d\tau}\Big|_{\tau=\tau_{\max}} = -dH'(\tau) + L'(\tau) - \frac{d\tilde{\lambda}}{d\tau}\big(H(\tau)+\tau L(\tau)\big)\Big|_{\tau=\tau_{\max}}.$$

Solving for $\frac{d\tilde{\lambda}}{d\tau}$ and taking the real part yields

$$\mathrm{Re}\left(\frac{d}{d\tau}\tilde{\lambda}\right)\Big|_{\tau=\tau_{max}} = \frac{d}{d\tau}\mathrm{Re}(\tilde{\lambda})\Big|_{\tau=\tau_{max}} = \frac{L'(\tau)-dH'(\tau)}{H(\tau)+\tau L(\tau)}\Big|_{\tau=\tau_{max}} = \frac{d^2}{\ln\left(\frac{cmK}{d(a+K)}\right)+1} > 0.$$

Hence, the real part of $\tilde{\lambda}$ changes sign at $\tau = \tau_{max}$ from negative to positive. This implies that E^* moves from the first quadrant to the fourth quadrant and changes stability from stable to unstable. Thus, E_K and E^* exchange stability at $\tau = \tau_{max}$, where they merge in a transcritical bifurcation. □

4. Global Hopf bifurcation and continuity of branches

By the local Hopf bifurcation Theorem 3.6 and Corollary 3.10, the periodic solutions bifurcating from E^* exist in a small neighbourhood of a sequence of critical values $\tau = \tau_n^{(i)}$ where $i = 1, 2, \cdots, \chi(n)$ and $n \in \mathbb{N}$. In this section, we study the evolution of periodic solutions as τ varies within $(0, \tau_{max})$. The global Hopf bifurcation theory developed by Wu is implemented (see Theorem 3.3 of [25]), and connected components of non-trivial periodic solutions in Fuller's space are considered. By estimating the period of the period solution and studying the τ-interval in which the period solution exists, we can describe the onset and termination of Hopf bifurcation branches under certain conditions.

Let $\tilde{x}(t) = x(t\tau)$, $\tilde{y}(t) = y(t\tau)$, then system (1.2) can be rewritten as

$$\dot{z} = F(z_t, \tau, T),\ (t, \tau, T) \in \mathbb{R}_+ \times (0, \tau_{max}) \times \mathbb{R}_+, \tag{4.1}$$

where

$$z(t) = \begin{bmatrix}\tilde{x}(t)\\ \tilde{y}(t)\end{bmatrix},\ F(z_t,\tau,T) = \begin{bmatrix}\tau r\tilde{x}(t)\left(1-\frac{\tilde{x}(t)}{K}\right) - \tau\frac{m\tilde{x}(t)\tilde{y}(t)}{a+\tilde{x}(t)}\\ -\tau d\tilde{y}(t) + \tau e^{-d\tau}\frac{cm\tilde{x}(t-1)\tilde{y}(t-1)}{a+\tilde{x}(t-1)}\end{bmatrix}.$$

Let $z_t(s) = z(t+s)$ for $s \in [-1, 0]$, so that $z_t \in C([-1, 0], \mathbb{R}^2_+)$. Hence, the domain of $F(z_t, \tau, T)$ is $C([-1, 0], \mathbb{R}^2_+) \times (0, \tau_{max}) \times \mathbb{R}_+$. By identifying the subspace of $C([-1, 0], \mathbb{R}^2_+)$ consisting of all constant mapping with $\mathbb{R}^2_+$, we obtain a restricted mapping

$$\tilde{F}(z,\tau,T) := F(z_t,\tau,T)_{|\mathbb{R}^2_+\times(0,\tau_{max})\times\mathbb{R}_+} = \begin{bmatrix}\tau r\tilde{x}\left(1-\frac{\tilde{x}}{K}\right) - \tau\frac{m\tilde{x}\tilde{y}}{a+\tilde{x}}\\ -\tau d\tilde{y} + \tau e^{-d\tau}\frac{cm\tilde{x}\tilde{y}}{a+\tilde{x}}\end{bmatrix}.$$

Then, $\tilde{F}$ is twice continuously differentiable, and condition (A1) of Theorem 3.3 of [25] is fulfilled.

https://doi.org/10.1017/S0956792526100370 Published online by Cambridge University Press

Let $\mathscr{N}(F) = \{(z, \tau, T) | \tilde{F}(z, \tau, T) = 0\}$ be the set of stationary solutions of system (4.1). From our analysis in Section 3, we know

$$\mathscr{N}(F) = \{(z, \tau, T) | z \in \{E_0, E_K, E^*\}, (\tau, T) \in (0, \tau_{max}) \times \mathbb{R}_+\}.$$

It is apparent that the function $F(z_t, \tau, T)$ is continuously differentiable with respect to its first argument z_t and the characteristics matrix function at the stationary solution $(z, \tau, T) \in \mathscr{N}(F)$ is

$$\Delta_{(z,\tau,T)}(\lambda) = \lambda Id - DF(z, \tau, T)(e^{\lambda \cdot} Id).$$

Here, $DF(z, \tau, T)$ is the complexification of the derivative of $F(z_t, \tau, T)$ with respect to z_t evaluated at $(z, \tau, T) \in \mathscr{N}(F)$. Since $\Delta_{(z,\tau,T)}$ is continuous, condition (A3) of Theorem 3.3 of [25] is fulfilled.

Furthermore, by Lemma 2.6 and Theorem 3.12, we establish that $\lambda = 0$ is not an eigenvalue of E_0, E_K, or E^* for $\tau \in (0, \tau_{max})$, meaning $\det(DF(z, \tau, T)) \neq 0$ for $(z, \tau, T) \in \mathscr{N}(F)$. Thus, $DF(z, \tau, T)$ is isomorphic to $\mathbb{R}^2$ at each stationary solution, and condition (A2) of Theorem 3.3 of [25] is fulfilled.

For the global Hopf bifurcation, by Lemma 2.1 and Theorem 3.6, $(E^*, \tau, T) \in \mathscr{N}(F)$ is the only stationary solution under consideration. Assume condition (H1) is satisfied, i.e., $S_n(\tau) = 0$ has $\chi(n)$ roots on $(0, \bar{\tau})$, where $\chi(n) < \infty, \forall n \in \mathbb{N}$, and these $\chi(n)$ roots are given and arranged in the following order

$$\tau_n^{(1)} < \tau_n^{(2)} < \cdots < \tau_n^{(i)} < \cdots \tau_n^{(\chi(n))}.$$

Furthermore, $\delta(\tau_n^{(i)}) = \pm 1$ $(i = 1, 2, \cdots, \chi(n))$.

By the definition of a centre for a stationary solution [25], the points

$$\left(E^*, \tau_n^{(i)}, \frac{2\pi}{\tau_n^{(i)} w(\tau_n^{(i)})}\right) = \left(E^*, \tau_n^{(i)}, \frac{2\pi}{\theta_n(\tau_n^{(i)})}\right), \ n \in \mathbb{N}, \ i = 1, 2, \cdots, \chi(n) \tag{4.2}$$

are centres of system (4.1). For each centre, it is the only centre in its small neighbourhood, and it only has finitely many purely imaginary characteristic values, whose imaginary part takes the form

$$\tau_n^{(i)} w\left(\tau_n^{(i)} = i \frac{2\pi}{2\pi/(\tau_n^{(i)} w(\tau_n^{(i)}))} = \frac{2\pi}{2\pi/(\theta_n(\tau_n^{(i)}))}.\right.$$

Here, $T_n^{(i)} := 2\pi/(\tau_n^{(i)} w(\tau_n^{(i)})) = 2\pi/(\theta_n(\tau_n^{(i)}))$ is the minimal period of periodic solution bifurcating at $\tau_n^{(i)}$ for the scaled model (4.1). Therefore, $(E^*, \tau_n^{(i)}, \frac{2\pi}{\theta(\tau_n^{(i)})})$ given in (4.2) are isolated centres. Moreover, the first crossing number of each isolated centre $\gamma_1(E^*, \tau_n^{(i)}, \frac{2\pi}{\theta(\tau_n^{(i)})})$ is well defined, and

$$\gamma_1\left(E^*, \tau_n^{(i)}, \frac{2\pi}{\theta(\tau_n^{(i)})}\right) = -\text{sign}\left(\frac{d}{d\tau} Re(\lambda)\big|_{\tau=\tau_n^{(i)}}\right) = -\text{sign}(S'(\tau_n^{(i)})) = -\delta(\tau_n^{(i)}) = \pm 1.$$

Hence, condition (A4) of Theorem 3.3 of [25] is fulfilled.

Define the closed set $\Sigma(F)$ in $C([-1, 0], \mathbb{R}_+^2) \times (0, \tau_{max}) \times \mathbb{R}_+$ as follows:

$$\Sigma(F) = Cl\{(z, \tau, T) \in C([-1, 0], \mathbb{R}_+^2) \times (0, \tau_{max}) \times \mathbb{R}_+ | z \text{ is a } T\text{-periodic solution of system (4.1)}\}.$$

Let $\mathscr{C}(E^*, \tau_n^{(i)}, \frac{2\pi}{\theta(\tau_n^{(i)})})$ be the connected component of $(E^*, \tau_n^{(i)}, \frac{2\pi}{\theta(\tau_n^{(i)})})$ in $\Sigma(F)$.

By ensuring that conditions (A1)-(A4) of Theorem 3.3 in [25] hold, we can now apply the global Hopf bifurcation theorem to system (4.1).

Theorem 4.1. *Consider the system (4.1) with (H1). One of the following two statements holds.*

(i) $\mathscr{C}(E^*, \tau_n^{(i)}, \frac{2\pi}{\theta(\tau_n^{(i)})})$ *is unbounded;*

(ii) $\mathscr{C}(E^*, \tau_n^{(i)}, \frac{2\pi}{\theta(\tau_n^{(i)})})$ *is bounded, the intersection* $\mathscr{C}(E^*, \tau_n^{(i)}, \frac{2\pi}{\theta(\tau_n^{(i)})}) \cap \mathscr{N}(F)$ *is finite, and*

$$\sum_{(z,\tau,T) \in \mathscr{C}\left(E^*, \tau_n^{(i)}, \frac{2\pi}{\theta(\tau_n^{(i)})}\right) \cap \mathscr{N}(F)} \gamma_1(z, \tau, T) = 0.$$

Here, $i = 1, 2, \cdots, \chi(n)$ *and* $n \in \mathbb{N}$.

https://doi.org/10.1017/S0956792526100370 Published online by Cambridge University Press

In the following, we analyse the boundedness and connections of $\mathscr{C}(E^*, \tau_n^{(i)}, \frac{2\pi}{\theta(\tau_n^{(i)})})$.

Lemma 4.2. *Let* $\Gamma := \{(\xi_1(t), \xi_2(t)) : t \in [0, \infty)\}$ *be any non-constant periodic solution of system (1.2) with initial condition* $\phi \in \mathbf{C} \times \mathbf{C}$. *Then* $0 < \xi_1(t) \le K, 0 < \xi_2(t) \le cK$, *for all* $t \ge 0$.

Proof. By Lemma 2.1, ξ_1 and ξ_2 are positive for all $t \ge 0$. By Lemma 2.2, we have $\limsup_{t\to\infty} x(t) \le K$. We assert that $\xi_1(t) \le K$ for all $t \ge 0$. If not, then there exists $t_1 > 0$ such that $\xi_1(t_1) > K$. Then,

$$K < \xi_1(t_1) = \lim_{n\to\infty} \xi_1(t_1 + nT) \le \limsup_{t\to\infty} \xi_1(t) \le K,$$

which is a contradiction. By a similar argument, we conclude that $\xi_2(t) \le cK$ for all $t \ge 0$. □

Lemma 4.3. *If* $K < K_0$, *system (4.1) has no periodic solutions of period 1.*

Proof. At a periodic solution with period 1, we have $\tilde{x}(t-1) = \tilde{x}(t)$ and $\tilde{y}(t-1) = \tilde{y}(t)$. To show that system (4.1) has no periodic solution of period 1, we replace $\tilde{x}(t-1)$ and $\tilde{y}(t-1)$ with $\tilde{x}(t)$ and $\tilde{y}(t)$, respectively, reducing system (4.1) to the ODE system

$$\begin{cases} \frac{d\tilde{x}}{dt} = \tau r\tilde{x}\left(1 - \frac{\tilde{x}}{K}\right) - \tau\frac{m\tilde{x}\tilde{y}}{a+\tilde{x}}, \\ \frac{d\tilde{y}}{dt} = \tau\tilde{y}\left(-d + ce^{-d\tau}\frac{m\tilde{x}}{a+\tilde{x}}\right). \end{cases} \tag{4.3}$$

By Lemma 2.4 and substituting c with $ce^{-d\tau}$, we obtain that system (4.3) does not have a periodic solution when $K < \frac{a(cme^{-d\tau}+d)}{cme^{-d\tau}-d}$. Notice that $K_0 = \frac{a(cm+d)}{cm-d} < \frac{a(cme^{-d\tau}+d)}{cme^{-d\tau}-d}$, and therefore system (4.3) has no periodic solutions if $K < K_0$. Consequently, system (4.1) has no periodic solutions of period 1. □

We have the estimate of $T_n^{(i)}$, the minimal period of periodic solution bifurcating at $\tau_n^{(i)}$ for the scaled model (4.1) below.

Lemma 4.4. *If* $K < K_0$, *then* $T_n^{(i)} \in (\frac{1}{n+1}, \frac{1}{n})$ *for* $i = 1, 2, \cdots, \chi(n)$ *and* $n = 1, 2, \cdots$.

Proof. By Lemma 3.5, we have $2n\pi + \zeta \le \theta_n(\tau_n^{(i)}) \le (2n+1)\pi$ for all $\tau \in [0, \bar{\tau}]$. Then

$$\frac{1}{n+1} = \frac{2\pi}{(2n+2)\pi} < \frac{2\pi}{(2n+1)\pi} \le T_n^{(i)} \le \frac{2\pi}{2n\pi+\zeta} < \frac{1}{n}.$$

□

Theorem 4.5. *For system (4.1),* E_K *is globally asymptotically stable for* $\tau \ge \tau_{max}$, *and periodic solutions exist only on* $(0, \tau_{max})$.

Proof. Consider the Lyapunov functional

$$V(\tilde{x}, \tilde{y}) = \tilde{x} - K - K\ln\frac{\tilde{x}}{K} + \frac{mK}{da}\tilde{y} + \tau\frac{cm^2Ke^{-d\tau}}{da}\int_{t-1}^{t}\frac{\tilde{x}(s)\tilde{y}(s)}{a+\tilde{x}(s)}ds.$$

By Lemma 2.1, $V(\tilde{x}, \tilde{y})$ is well-defined. Furthermore, $V(\tilde{x}, \tilde{y}) \ge 0$ for all $\tilde{x} > 0, \tilde{y} \ge 0$, and $V(\tilde{x}, \tilde{y}) = 0$ if and only if $(\tilde{x}, \tilde{y}) = (K, 0)$, we compute the total derivative along system (4.1) with respect to t:

$$\begin{aligned} \dot{V}(\tilde{x}, \tilde{y}) &= r\tau\tilde{x}(t)\left(1 - \frac{\tilde{x}(t)}{K}\right) - \tau\frac{m\tilde{x}(t)\tilde{y}(t)}{a+\tilde{x}(t)} - K\tau\left(r\left(1 - \frac{\tilde{x}(t)}{K}\right) - \frac{m\tilde{y}(t)}{a+\tilde{x}(t)}\right) \\ &\quad + \tau\frac{cm^2Ke^{-d\tau}}{da}\cdot\frac{\tilde{x}(t-1)\tilde{y}(t-1)}{a+\tilde{x}(t-1)} - \tau\frac{mK}{a}\tilde{y}(t) \\ &\quad + \tau\frac{cm^2Ke^{-d\tau}}{da}\cdot\frac{\tilde{x}(t)\tilde{y}(t)}{a+\tilde{x}(t)} - \tau\frac{cm^2Ke^{-d\tau}}{da}\cdot\frac{\tilde{x}(t-1)\tilde{y}(t-1)}{a+\tilde{x}(t-1)} \\ &= \tau\left[-\frac{r}{K}(K-\tilde{x})^2 + \tilde{y}\left(\frac{-m\tilde{x}+Km}{a+\tilde{x}} - \frac{mK}{a} + \frac{cm^2Ke^{-d\tau}\tilde{x}}{da(a+\tilde{x})}\right)\right]. \end{aligned}$$

https://doi.org/10.1017/S0956792526100370 Published online by Cambridge University Press

For $\tau \geq \tau_{max}$, we obtain

$$\dot{V}(\tilde{x},\tilde{y}) \leq \tau\left[-\frac{r}{K}(K-\tilde{x})^2+\tilde{y}\left(\frac{-m\tilde{x}+Km}{a+\tilde{x}}-\frac{mK}{a}+\frac{cm^2Ke^{-d\tau_{max}}\tilde{x}}{da(a+\tilde{x})}\right)\right]$$
$$=-\frac{\tau r}{K}(K-\tilde{x})^2\leq 0.$$

The last equality holds if and only if $\tilde{x}=K$ and $\tilde{y}\geq 0$. From the first equation of system (4.1), the largest invariant set of $\{(K,\tilde{y})|\tilde{y}\geq 0\}$ is the singleton $\{(K,0)\}$. By Lyapunov–LaSalle's invariance principle [14], $(K,0)$ is globally asymptotically stable for $\tau \geq \tau_{max}$. □

Theorem 4.6. *Consider system (4.1), under the assumption (H1) with $K<K_0$. Then the following two statements hold.*

(1) *All connected components $\mathscr{C}(E^*,\tau_n^{(i)},\frac{2\pi}{\theta(\tau_n^{(i)})})$ are bounded for all $n=1,2,\cdots$.*

(2) *If $\chi(n)=2$, denote $\tau_n^{(1)}$ and $\tau_n^{(2)}$ as τ_n^- and τ_n^+, respectively. Then the connected components $\mathscr{C}(E^*,\tau_n^-,\frac{2\pi}{\theta(\tau_n^-)})$ and $\mathscr{C}(E^*,\tau_n^+,\frac{2\pi}{\theta(\tau_n^+)})$ coincide and are nested. The connected component $\mathscr{C}(E^*,\tau_n^\pm,\frac{2\pi}{\theta(\tau_n^\pm)})$ connects exactly two bifurcation points τ_n^- and τ_n^+, where $n=1,2,\cdots$.*

Proof. (1). By Lemma 4.2, all periodic solutions of system (4.1) are uniformly bounded. Therefore, the projection of $\mathscr{C}(E^*,\tau_n^{(i)},\frac{2\pi}{\theta(\tau_n^{(i)})})$ onto $C([-1,0],\mathbb{R}^2_+)$ is bounded.

By Lemmas 2.4 and 4.5, no periodic solution exists for $\tau=0$ or $\tau\geq\tau_{max}$. Consequently, the connected components do not extend beyond the finite interval $(0,\tau_{max})$. Hence, the projection of $\mathscr{C}(E^*,\tau_n^{(i)},\frac{2\pi}{\theta(\tau_n^{(i)})})$ onto τ-space is bounded.

Furthermore, by Lemma 4.3, there are no periodic solutions of period 1, and consequently, none with period $\frac{1}{n}, n=1,2,\cdots$. By the continuity of the connected component, the projection of $\mathscr{C}(E^*,\tau_n^{(i)},\frac{2\pi}{\theta(\tau_n^{(i)})})$ onto the T-space is a subset of the finite interval $(\frac{1}{n+1},\frac{1}{n})$. Hence, all connected components $\mathscr{C}(E^*,\tau_n^{(i)},\frac{2\pi}{\theta(\tau_n^{(i)})})$ are bounded in Fuller's space, where $n=1,2,\cdots$.

(2). By Lemma 4.4, the minimal period of the periodic solution bifurcating at $\tau_n^\pm$ is $T_n^\pm=\frac{2\pi}{\theta(\tau_n^\pm)}\in(\frac{1}{n+1},\frac{1}{n})$. By Lemma 4.3, the projection of $\mathscr{C}(E^*,\tau_n^\pm,\frac{2\pi}{\theta(\tau_n^\pm)})$ onto the T-space is a subset of the finite interval $(\frac{1}{n+1},\frac{1}{n})$. Moreover, $\mathscr{C}(E^*,\tau_n^-,\frac{2\pi}{\theta(\tau_n^-)})$ and $\mathscr{C}(E^*,\tau_n^+,\frac{2\pi}{\theta(\tau_n^+)})$ are the only two connected components whose third arguments belong to $(\frac{1}{n+1},\frac{1}{n})$.

By Theorem 4.1, the first crossing number of $(E^*,\tau_n^\pm,\frac{2\pi}{\theta(\tau_n^\pm)})$ on $\mathscr{C}(E^*,\tau_n^\pm,\frac{2\pi}{\theta(\tau_n^\pm)})$ satisfies

$$\sum_{(z,\tau,T)\in\mathscr{C}(E^*,\tau_n^\pm,\frac{2\pi}{\theta(\tau_n^\pm)})\cap\mathscr{N}(F)}\gamma_1(z,\tau,T)=0.$$

Note that

$$\gamma_1\left(E^*,\tau_n^-,\frac{2\pi}{\theta(\tau_n^-)}\right)=-1,\ \text{and}\ \gamma_1\left(E^*,\tau_n^+,\frac{2\pi}{\theta(\tau_n^+)}\right)=1.$$

Hence, $\mathscr{C}(E^*,\tau_n^-,\frac{2\pi}{\theta(\tau_n^-)})$ and $\mathscr{C}(E^*,\tau_n^+,\frac{2\pi}{\theta(\tau_n^+)})$ must coincide, initiating at $\tau=\tau_n^-$ and terminating at τ_n^+ in the τ-space (or vice versa). Since $\tau_j^-<\tau_i^-<\tau_i^+<\tau_j^+$ for $j<i$, the components $\mathscr{C}(E^*,\tau_n^\pm,\frac{2\pi}{\theta(\tau_n^\pm)})$ are nested, where $n=1,2,\cdots$. □

If $\chi(0)=2$ and assume the projection of $\mathscr{C}(E^*,\tau_0^-,\frac{2\pi}{\theta(\tau_0^-)})$ and $\mathscr{C}(E^*,\tau_0^+,\frac{2\pi}{\theta(\tau_0^+)})$ onto the T-space are bounded, by Theorem 4.1 and a similar argument as that of Theorem 4.6, we obtain the following result.

Theorem 4.7. *Let $K<K_0$ and $\chi(0)=2$. If the projection of $\mathscr{C}(E^*,\tau_0^-,\frac{2\pi}{\theta(\tau_0^-)})$ and $\mathscr{C}(E^*,\tau_0^+,\frac{2\pi}{\theta(\tau_0^+)})$ onto the T-space are bounded, then they coincide and connect two bifurcation points τ_0^- and τ_0^+.*

Proof. By Lemma 4.2, all periodic solutions of system (4.1) are uniformly bounded. Therefore, the projection of $\mathscr{C}(E^*,\tau_0^\pm,\frac{2\pi}{\theta(\tau_0^\pm)})$ onto $C([-1,0],\mathbb{R}^2_+)$ is bounded. By Lemmas 2.4 and 4.5, no periodic solution

https://doi.org/10.1017/S0956792526100370 Published online by Cambridge University Press

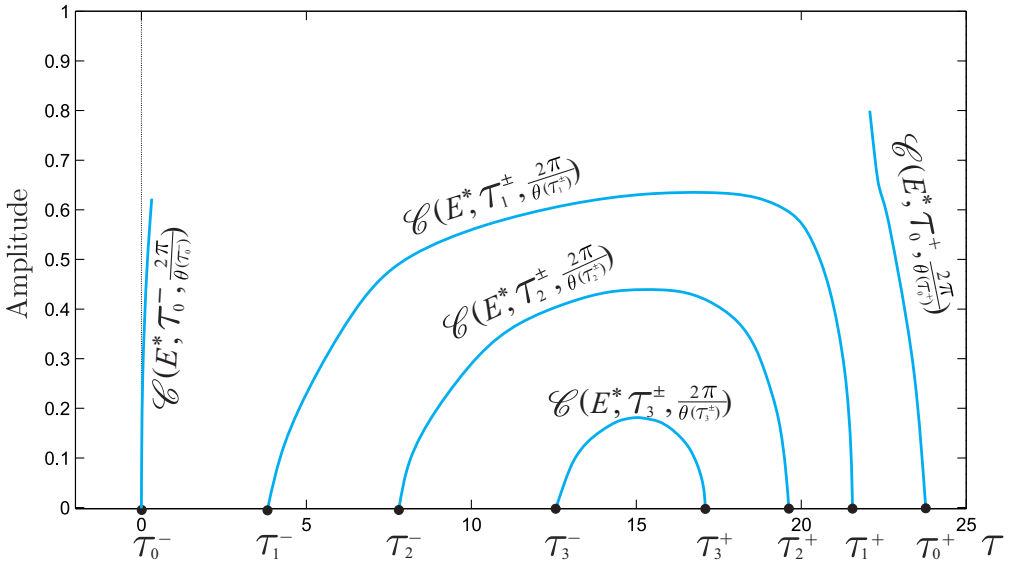


Figure 3. *Global Hopf bifurcation and connected components for $K < K_0$. The parameters and values of $\tau_n^\pm (n = 0, 1, 2, 3)$ are provided in Example 1(a).*

extends beyond the interval $(0, \tau_{\max})$, so the projection of $\mathscr{C}(E^*, \tau_0^\pm, \frac{2\pi}{\theta(\tau_0^\pm)})$ onto τ-space is bounded. It follows from the assumption that $\mathscr{C}(E^*, \tau_0^-, \frac{2\pi}{\theta(\tau_0^-)})$ and $\mathscr{C}(E^*, \tau_0^+, \frac{2\pi}{\theta(\tau_0^+)})$ are the only two connected components whose third components lie in a bounded subset of $(1, \infty)$, and the product of their first crossing numbers satisfies

$$\gamma_1\left(E^*, \tau_0^-, \frac{2\pi}{\theta(\tau_0^-)}\right) \cdot \gamma_1\left(E^*, \tau_0^+, \frac{2\pi}{\theta(\tau_0^+)}\right) = -1.$$

Therefore, by Theorem 4.1, the two components $\mathscr{C}\big(E^*, \tau_0^-, \frac{2\pi}{\theta(\tau_0^-)}\big)$ and $\mathscr{C}\big(E^*, \tau_0^+, \frac{2\pi}{\theta(\tau_0^+)}\big)$ coincide and connect two bifurcation points τ_0^- and τ_0^+. □

It is important to note that the nonexistence of periodic solutions in the ODE system (2.1) (i.e., system (1.2) plays a crucial role in establishing the boundedness and connectedness of the connected components, as demonstrated in the proof of Theorem 4.6. However, when $K > K_0$, system (1.2) admits a periodic solution at $\tau = 0$. Consequently, system (4.1) also possesses a periodic solution of period 1. As a result, we lose the ability to estimate the period of the connected components in the T-space, and whether $\mathscr{C}(E^*, \tau_n^-, \frac{2\pi}{\theta(\tau_n^-)})$ and $\mathscr{C}(E^*, \tau_n^+, \frac{2\pi}{\theta(\tau_n^+)})$ coincide remains unclear if $\chi(n) = 2$ (see Figure 3 for these two connected components. It is not clear whether they are connected due to the computational challenge).

Nevertheless, we will explore the relations between the connected components for $K > K_0$ through numerical analysis using *DDE-BifTool*. Instead of analysing $\mathscr{C}(E^*, \tau_n^{(i)}, \frac{2\pi}{\theta(\tau_n^{(i)})})$ for system (4.1), we consider the connected components $\mathscr{C}(E^*, \tau_n^{(i)}, \frac{2\pi}{w(\tau_n^{(i)})})$ for system (1.2), since a periodic solution exists at $\tau = 0$.

- *A unique connected component and the limit cycle of the ODE model (2.1).*
  If $\chi(0) = 1$ and $\chi(n) = 0$ for $n \geq 1$, $S_0(\tau) = 0$ has a unique root $\tau = \tau_0^{(1)}$ on $[0, \bar{\tau})$ and system (1.2) has a unique connected component $\mathscr{C}(E^*, \tau_0^{(1)}, \frac{2\pi}{w(\tau_0^{(1)})})$. When $\tau = 0$, $J(E^*)$ has a pair of conjugate complex eigenvalues with positive real part, meaning E^* is unstable and a stable limit cycle Γ_0 (i.e, an isolated periodic solution) exists around E^*. As τ increases from 0 to $\tau_0^{(1)}$, and passes by $\tau_0^{(1)}$, Lemma 3.1 implies that this pair of complex eigenvalues vary continuously, crossing the imaginary axis from

https://doi.org/10.1017/S0956792526100370 Published online by Cambridge University Press

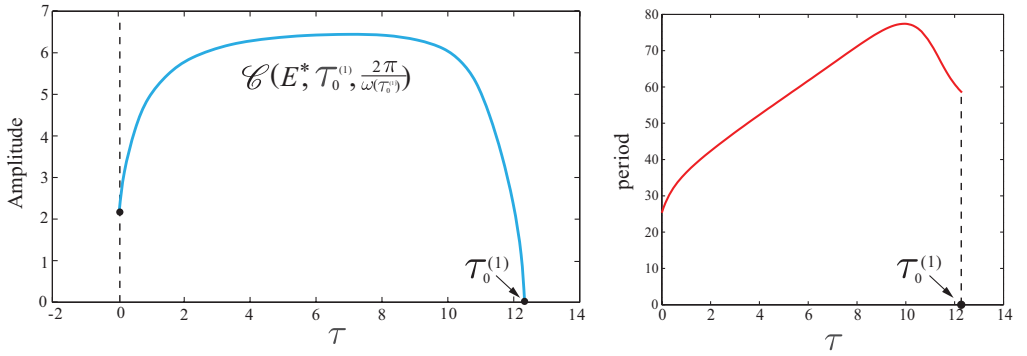


Figure 4. *Global Hopf bifurcation and a unique connected component $\mathscr{C}(E^*, \tau_0^{(1)}, 2\pi/w(\tau_0^{(1)}))$ for $K > K_0$. The left panel shows the amplitude and the right panel displays the period of the periodic solution for $\tau \in [0, \tau_0^{(1)}]$. The parameter are $K = 7, r = 1, m = 1, c = 1, d = 0.1, a = 5$, and $K > K_0 = 6.11$.*

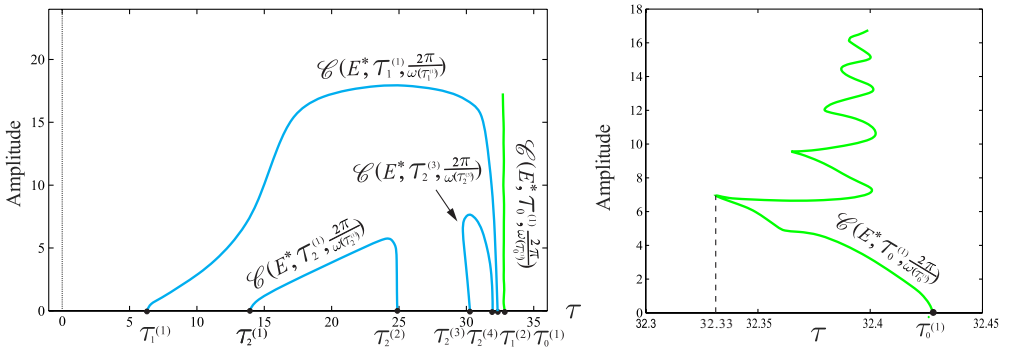


Figure 5. *Global Hopf bifurcation and multiple connected components for $K > K_0$. The right panel is a magnified view of the left panel near $\tau = \tau_0^{(1)}$. The parameter values and $\tau_n^{(i)} (n = 0, 1, 2)$ are specified in Example 1(b).*

right to left at $\tau = \tau_0^{(1)}$ so that E^* becomes stable. Meanwhile, the limit cycle Γ_0 evolves continuously. However, Γ_0 does not necessarily persist over the entire interval $[0, \tau_0^{(1)})$, as it may vanish due to a bifurcation of periodic solutions at some $\tau < \tau_0^{(1)}$. If no such bifurcation occurs for $\tau \in (0, \tau_0^{(1)})$, then Γ_0 must disappear through a local Hopf bifurcation at $\tau = \tau_0^{(1)}$, i.e., $(\Gamma_0, 0, \frac{2\pi}{\bar{w}}) \in \mathscr{C}(E^*, \tau_0^{(1)}, \frac{2\pi}{w(\tau_0^{(1)})})$, where $\bar{w}$ is the frequency of the limit cycle Γ_0.Thus, *the limit cycle of the ODE model (2.1) belongs to a connected component of the Hopf bifurcation of the DDE model (1.2) in Fuller's space*. As illustrated in Figure 4, Γ_0 varies continuously on $[0, \tau_0^{(1)}]$ and terminates $\tau = \tau_0^{(1)}$ through a Hopf bifurcation.

- *Multiple connected components.*
  If $\chi(n) > 2$ for some $n \in \mathbb{N}$, then $S_n(\tau) = 0$ has $\chi(n)$ critical values $\tau = \tau_n^{(i)}$, leading to $\chi(n)$ connected components $\mathscr{C}(E^*, \tau_n^{(i)}, \frac{2\pi}{\theta(\tau_n^{(i)})})$, where $i = 1, 2, \cdots, \chi(n)$. Studying the relationship between these connected components is technically challenging, regardless of whether $K < K_0$ or $K > K_0$. To illustrate this complexity, we consider the parameter values from Example 1(b), where $\chi(0) = 1, \chi(1) = 2, \chi(2) = 4$, and $\chi(n) = 0$ for $n \geq 3$. Based on Figure 5 we have the following observations:
  - For $n = 0$: $\mathscr{C}(E^*, \tau_0^{(1)}, \frac{2\pi}{w(\tau_0^{(1)})})$ initials at $\tau_0^{(1)}$, and experiences a sequence of saddle-node bifurcations of limit cycles occurs in the interval $[32.33, 32.4]$. The curve does not extend any further due to computational challenges.

https://doi.org/10.1017/S0956792526100370 Published online by Cambridge University Press

– For $n=1$: $\mathscr{C}(E^*, \tau_1^{(1)}, \frac{2\pi}{w(\tau_1^{(1)})})$ and $\mathscr{C}(E^*, \tau_1^{(2)}, \frac{2\pi}{w(\tau_1^{(2)})})$ coincide, i.e., the periodic solution initials at $\tau_1^{(1)}$ and terminates at $\tau_1^{(2)}$.
– For $n=2$: $\mathscr{C}(E^*, \tau_2^{(1)}, \frac{2\pi}{w(\tau_2^{(1)})})$ and $\mathscr{C}(E^*, \tau_2^{(2)}, \frac{2\pi}{w(\tau_2^{(2)})})$ coincide, $\mathscr{C}(E^*, \tau_2^{(3)}, \frac{2\pi}{w(\tau_2^{(3)})})$ and $\mathscr{C}(E^*, \tau_2^{(4)}, \frac{2\pi}{w(\tau_2^{(4)})})$ coincide. That is to say, we have the formation of a periodic solution at $\tau_2^{(1)}$ terminating at $\tau_2^{(2)}$, and a formation of another periodic solution at $\tau_2^{(3)}$ terminating at $\tau_2^{(4)}$.

5. Bifurcation diagram

In this section, we examine the bifurcation diagram of system (1.2) in the (τ, K)-plane. By statement (2) of Lemma 3.12, a transcritical bifurcation involving E_K and E^* occurs when $\tau = \tau_{max}$, i.e., (τ, K) lies on the curve $\mathscr{L}_c$, defined as

$$\mathscr{L}_c := \left\{ (\tau, K) \in \overline{\mathbb{R}}_+ \times \mathbb{R}_+ | K = \frac{ad}{cme^{-d\tau} - d} \right\}.$$

By Corollary 3.10, there exists a sequence of bifurcation curves through which Hopf bifurcation occurs at E^*. Let $\ell_n(\tau, K) := \tau w(\tau, K) - \theta_n(\tau.K)$. The Hopf bifurcation curve is given by

$$\mathscr{L}_n = \{(\tau, K) \in \overline{\mathbb{R}}_+ \times \mathbb{R}_+ | \ell_n(\tau, K) = 0, 0 \le \tau < \bar{\tau}\},\ n = 0, 1, 2, \cdots.$$

Lemma 5.1. *Consider the curve $\mathscr{L}_0$, i.e., the graph of $\ell_0(\tau, K) = 0$.*

(1) *$\mathscr{L}_0$ lies above the curve $\mathscr{L}_c$.*
(2) *$\mathscr{L}_0$ starts at the point $(\tau, K) = (0, K_0)$ and extends to infinity, meaning $\mathscr{L}_0$ exists for all $K \ge K_0$.*
(3) *There exists a smooth function $K = K(\tau)$ for $\tau \in [0, \varepsilon)$, where $\varepsilon > 0$ is small such that*

$$K_0 = K(0), \quad \ell_0(K(\tau), \tau) = 0, \ \tau \in [0, \varepsilon).$$

Furthermore, $K'(\tau) < 0$ if $cm > (1+\sqrt{2})d$, $K'(\tau) > 0$ if $cm < (1+\sqrt{2})d$. If $cm = (1+\sqrt{2})d$, then $K''(\tau) > 0$.

Proof. Statement (1) follows directly from Lemma 2.5.

(2) Since $\ell_0(0, K_0) = 0 - \arccos(1) = 0$, the point $(0, K_0)$ serves as an endpoint of $\mathscr{L}_0$. By Lemma 3.4, for any $K \ge K_0$, $\tau w(\tau)$ intersects $\theta_0(\tau)$ at least once. Hence, the graph of $\ell_0(\tau, K) = 0$ exists for all $K \ge K_0$.

(3) By direct calculation, we obtain

$$\ell_0(0, K_0) = 0, \text{ and } \frac{\partial \ell_0(\tau, K)}{\partial K}_{|(0,K_0)} = -\frac{(cm-d)\sqrt{rd}}{mca\sqrt{c^2m^2 - d^2}} \neq 0.$$

By the implicit function theorem, there exists a function $K = K(\tau)$ for $\tau \in [0, \varepsilon)$, where $\varepsilon > 0$ is small such that $K_0 = K(0)$ and $\ell_0(K(\tau), \tau) = 0$. Furthermore, a straightforward calculation yields

$$K'(\tau)_{|\tau=0} = -\frac{mca(c^2m^2 - 2cmd - d^2)}{(cm-d)^2}.$$

If $K'(\tau)_{|\tau=0} = 0$ (i.e., $cm = (1+\sqrt{2})d$), then by implicit differentiation, $K''(\tau)_{|\tau=0} = 3\sqrt{2}ac^2m^2$. This establishes the desired result. □

In what follows, we will sketch the bifurcation diagram of the system (1.2) in the first quadrant of the (τ, K) plane. There are a curve of transcritical bifurcation $\mathscr{L}_c$ and a curve of Hopf bifurcation $\mathscr{L}_0$. By statement (3) of Lemma 5.1, in a neighbourhood of $(0, K_0)$, the curve $\mathscr{L}_0$ exhibits different monotonicity behaviours depending on whether $cm \le (1+\sqrt{2})d$ or $cm > (1+\sqrt{2})d$. The simplest sketch of $\mathscr{L}_0$ is presented in Figure 6, ensuring minimal changes in monotonicity for $\tau \in [0, \check{\tau})$.

https://doi.org/10.1017/S0956792526100370 Published online by Cambridge University Press

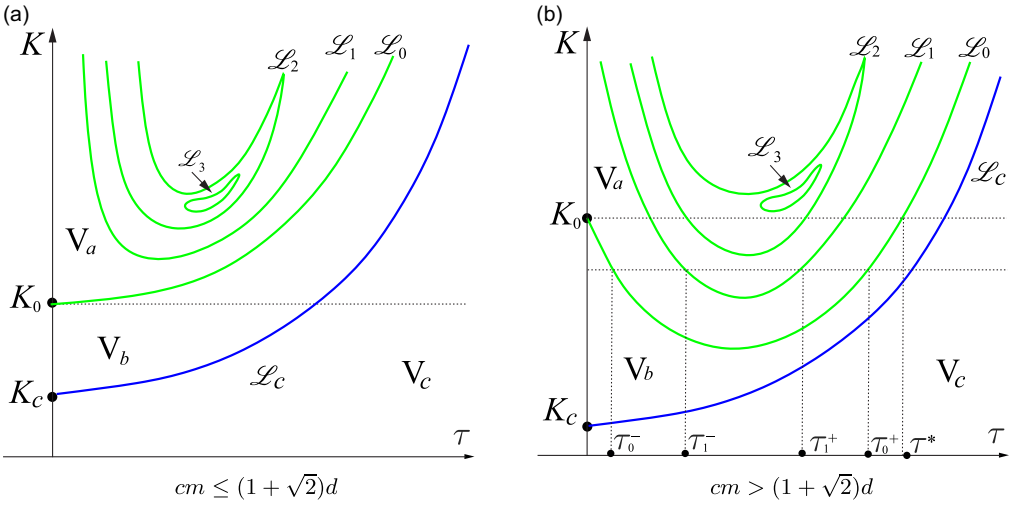


Figure 6. *Bifurcation diagram in the (τ, K)-plane. The curve $\mathscr{L}_c$ represents the transcritical bifurcation, while $\mathscr{L}_n (n = 0, 1, 2, 3)$ are curves of Hopf bifurcation. Dash lines highlight critical parameter values that are not bifurcation curves.*

The two curves $\mathscr{L}_c$ and $\mathscr{L}_0$ divide the first quadrant of (τ, K)-plane into three regions V_a, V_b, and V_c, defined as follows:

$$V_a = \{(\tau, K) \in \overline{\mathbb{R}}_+ \times \mathbb{R}_+ | \ell_0(\tau, K) >, 0 \leq \tau < \bar{\tau}\},$$
$$V_b = \{(\tau, K) \in \overline{\mathbb{R}}_+ \times \mathbb{R}_+ | \ell_0(\tau, K) < 0, 0 \leq \tau < \bar{\tau}\}, V_c = \{(\tau, K) \in \overline{\mathbb{R}}_+ \times \mathbb{R}_+ | \tau > \tau_{max}\}.$$

By Theorem 4.5, E_K is globally asymptotically stable for $(K, \tau) \in V_c$, and system (1.2) undergoes a transcritical bifurcation for $(K, \tau) \in \mathscr{L}_c$. E^* is locally asymptotically stable for $(K, \tau) \in V_b$, then system (1.2) experiences a Hopf bifurcation for $(K, \tau) \in \mathscr{L}_0$. E^* is unstable for $(K, \tau) \in V_a$, and a periodic solution exists for (K, τ) in a tubular neighbourhood of $\mathscr{L}_0$.

The existence of additional Hopf bifurcation curves $\mathscr{L}_n (n = 1, 2, \cdots)$ depends on the choice of parameters. If such curves exist, they are positioned above $\mathscr{L}_0$ and do not intersect any other Hopf bifurcation curve. Numerical studies suggest two possible topological structures for $\mathscr{L}_n$: $\mathscr{L}_n \simeq \mathbb{R}$, or $\mathscr{L}_n \simeq \mathbb{S}^1$, where $\simeq$ means "is topologically isomorphic". Figure 6 illustrates an example where $\mathscr{L}_1 \simeq \mathbb{R}$, $\mathscr{L}_2 \simeq \mathbb{R}$, $\mathscr{L}_3 \simeq \mathbb{S}^1$.

The region V_a is divided into several subregions by the Hopf bifurcation curves $\mathscr{L}_n (n = 1, 2, \cdots)$. Whenever (K, τ) crosses $\mathscr{L}_n$, the Hopf bifurcation occurs, and a periodic solution emerges in a tubular neighbourhood of $\mathscr{L}_n$. For $K < K_0$, if $\mathscr{L}_n (n = 2, 3, \cdots)$ transversally intersects the horizontal line exactly twice, by Theorem 4.6, the connected components $\mathscr{C}(E^*, \tau_n^-, \frac{2\pi}{w(\tau_n^-)})$ and $\mathscr{C}(E^*, \tau_n^+, \frac{2\pi}{w(\tau_n^+)})$ coincide. That is, a periodic solution emerging at (τ_n^-, K) will terminate at (τ_n^+, K). Determining the number of periodic solutions within the subregions between successive Hopf bifurcation curves is challenging. This is due to the potential presence of other bifurcations affecting periodic solutions. Even in the absence of such bifurcations, tracing the periodic solutions as (τ, K) crosses $\mathscr{L}_n (n = 0, 1, 2 \cdots)$ remains difficult, as there is no definitive criterion for predicting the onset and termination of connected components in global Hopf bifurcation when $K > K_0$ or $\chi(n) > 2$.

Remark 5.2. *The bifurcation diagram in Figure 6 is not complete, as there may exist additional bifurcation curves of periodic solutions, such as saddle-node bifurcations of limit cycles and period-doubling bifurcations. A detailed investigation of these bifurcations is beyond the scope of this work.*

https://doi.org/10.1017/S0956792526100370 Published online by Cambridge University Press

Remark 5.3. *If* $cm > (1+\sqrt{2})d$, *define*

$$\tau^* = \arg\min_{\tau\in(0,\bar{\tau})}\{\ell_0(\tau, K_0) = 0\}.$$

Then, for any point $(\tau, K) \in \mathscr{L}_0$ *with* $0 < \tau < \tau^*$, *we have* $K < K_0$ *(see Figure 6 (b)).*

Biological significance of τ^***.** *Predator–prey coexistence via oscillatory patterns can occur at lower environmental carrying capacities when delay* ($\tau > 0$) *is introduced, compared to scenarios without delay* ($\tau = 0$) *under the condition that* $(1+\sqrt{2})d < cm$, *and* $0 < \tau < \tau^*$. The significance of τ^* will be further illustrated in the next section.

6. Discussion

The classical predator–prey model with Holling type II functional response typically exhibits relatively simple dynamical behaviour. By contrast, the incorporation of a maturation delay introduces significantly richer dynamics and provides a more realistic framework for modelling predator–prey interactions observed in nature. In this section, we interpret the effects of delay on population persistence and oscillatory coexistence.

- *Threshold dynamics for prey–predator coexistence.*
  The coexistence of prey and predators requires $\tau < \tau_{\max}$, which is equivalent to $K > K_1$. Here

  $$K_1 = \frac{ad}{cme^{-d\tau} - d},$$

  and thus

  $$K_1 > \frac{ad}{cme^{-d\tau} - d}\Big|_{\tau=0} = K_c.$$

  As τ increases, K_1 increases, meaning that a higher environmental carrying capacity is needed for both species to coexist. This threshold is illustrated by the transcritical bifurcation curve $\mathscr{L}_c$ in Figure 6, together with the critical values K_1 and K_c shown in Figure 7. Biologically, this behaviour is intuitive: larger delays reduce predator survival ($e^{-d\tau}$), forcing predators to rely on greater prey abundance to compensate for mortality. As a consequence, prey populations face stronger predation pressure.
- *Oscillatory dynamics of prey and predator populations.*
  Oscillatory dynamics emerge once the condition $\ell_0(\tau, K) > 0$ is satisfied. A secondary threshold involving the predator death rate further determines whether sustained oscillations are possible.
  1. If $cm \le (1+\sqrt{2})d$, predator mortality is relatively high, leading to low survival $e^{-d\tau}$. In this case, predators require more prey to maintain oscillations. Since survival decreases as τ increases, the critical carrying capacity rises monotonically with τ. This behaviour is reflected by the monotone increase of $\mathscr{L}_0$ in Figure 6(a).
  2. If $cm > (1+\sqrt{2})d$, predator mortality is comparatively low, yielding higher survival rates. For small delays $\tau \in (0, \tau^*)$, oscillatory coexistence can be sustained at lower values of K. However, once τ exceeds τ^* (with $\tau \in (\tau^*, \bar{\tau})$), survival declines sufficiently to require larger K values for oscillations to persist. This non-monotone behaviour of $\mathscr{L}_0$ is illustrated in Figure 6(b), with τ^* defined in Remark 5.3.

To illustrate these effects, consider the bifurcation diagram of Figure 7, where K is treated as the bifurcation parameter. Fixing $\tau = 26$, $r = 30$, $m = 1$, $c = 4$, $d = 0.1$, and $a = 1$, we have $cm > (1+\sqrt{2})d$ and $\tau > \tau^* = 24.1$. The critical bifurcation values are

$$K_c = 0.25, \quad K_1 = 0.51, \quad K_0 = 1.0512, \quad K_h^{(1)} = 1.328, \quad K_h^{(2)} = 1.54, \quad K_h^{(3)} = 1.67, \quad K_h^{(4)} = 1.76,$$
$$K_h^{(5)} = 1.85, \quad K_h^{(6)} = 1.994, \quad K_h^{(7)} = 2.135, \quad K_h^{(8)} = 2.3956, \quad K_h^{(9)} = 2.7395, \quad K_h^{(10)} = 3.996.$$

https://doi.org/10.1017/S0956792526100370 Published online by Cambridge University Press

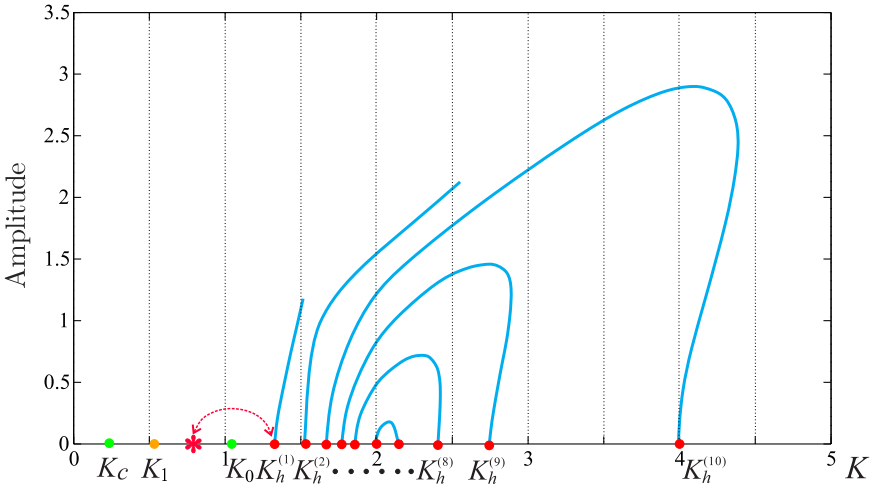


Figure 7. *Global Hopf bifurcation and connected components as functions of K for $\tau > \tau^*$. The orange dot corresponds to the transcritical bifurcation threshold K_1, while the red dots denote the Hopf bifurcation thresholds $K_h^{(i)}$ ($i = 1, 2, \ldots, 10$). The location of $K_h^{(1)}$ for $\tau \in (0, \tau^*)$ is indicated by "$*$". Critical values K_c and K_0 denote the transcritical and Hopf bifurcation thresholds of the ODE model ($\tau = 0$). Detailed descriptions are provided in this section.*

As K increases, system (1.2) undergoes a transcritical bifurcation at $K = K_1$ and a sequence of Hopf bifurcations at $K = K_h^{(i)}$. In particular, $K_h^{(1)} > K_0$ and $K_1 > K_c$, showing that delay increases the environmental resources needed for both coexistence and oscillatory dynamics.

When τ decreases into the interval $\tau \in (0, \tau^*)$, the first Hopf bifurcation threshold $K_h^{(1)}$ shifts to the position marked "$*$" between K_1 and K_0 in Figure 7. This indicates that smaller delays may allow oscillatory coexistence with fewer resources.

In summary, our results show that maturation delay is not uniformly detrimental. While increasing delay generally reduces effective recruitment through mortality during development (captured by the survival factor $e^{-d\tau}$), we also identify a counterintuitive regime in which *small* delays can *promote* predator persistence by enabling oscillatory coexistence at lower carrying capacities. This switch is organized by a critical timescale τ^*, which separates two qualitatively different outcomes: for $\tau > \tau^*$ the demographic cost dominates and delay increases the carrying-capacity requirements for both predator persistence and sustained oscillations, whereas for $\tau \in (0, \tau^*)$ modest delay can facilitate cyclic coexistence under tighter resource constraints.

A plausible explanation for this counterintuitive behaviour arises when $cm > (1 + \sqrt{2})d$. In the delay-free model, predator recruitment is strongly and nearly instantaneously coupled to current prey abundance, which stabilizes the coexistence equilibrium over a broad parameter range and postpones oscillations until enrichment is sufficiently large (in particular, until K exceeds K_0). Introducing a small maturation delay weakens this tight coupling by spreading recruitment over recent past prey conditions. Biologically, predator reproduction becomes less synchronized with current prey density and more influenced by prey availability during the recent past. As a result, the predator response is effectively smoothed and shifted in time: recruitment rises more slowly when prey increase and can remain elevated briefly after prey begin to decline. This timing shift can destabilize an equilibrium that is stable without delay, thereby generating self-sustained oscillations without requiring as much enrichment. Beyond τ^*, however, further delay increasingly penalizes recruitment, and the system again requires higher carrying capacity to sustain oscillations and maintain predator persistence.

https://doi.org/10.1017/S0956792526100370 Published online by Cambridge University Press

Acknowledgements. The authors would like to thank two anonymous referees for careful reading and insightful comments, which greatly improve the manuscript. We used ChatGPT to polish some of the writing.

Funding statement. The research of C. Shan was partially supported by Simons Foundation-Collaboration Grants for Mathematicians 523360. The research of H. Wang was partially supported by the Natural Sciences and Engineering Research Council of Canada (Individual Discovery Grant RGPIN-2025-05734 and Discovery Accelerator Supplement Award RGPAS-2020-00090) and the Canada Research Chairs program (Tier 1 Canada Research Chair Award).

Competing interests. The authors declare that they have no conflicts of interest.

References

[1] Armstrong, R. A. & McGehee, R. (1980) Competitive exclusion. *Am. Nat.* **115**, 151–170.
[2] Arino, J., Wang, L. & Wolkowicz, G. S. K. (2006) An alternative formulation for a delayed logistic equation. *J. Theoret. Biol.* **241**, 109–119.
[3] Beretta, E. & Kuang, Y. (2002) Geometric stability switch criteria in delay differential systems with delay dependent parameters. *SIAM J. Math. Anal.* **33**, 1144–1165.
[4] Cooke, K. L., van den Driessche, P. & Zou, X. (1999) Interaction of maturation delay and nonlinear birth in population and epidemic models. *J. Math. Biol.* **39**, 332–352.
[5] Cooke, J. K. L., Elderkin, R. H. & Huang, W. (2006) Predator–prey interactions with delays due to juvenile maturation. *SIAM J. Appl. Math.* **66**, 1050–1079.
[6] Fan, G. & Wolkowicz, G. S. (2021) Chaotic dynamics in a simple predator–prey model with discrete delay. *Discrete Contin. Dyn. Syst. Ser. B* **26**, 191–216.
[7] Gourley, S. A. & Kuang, Y. (2004) A stage structured predator–prey model and its dependence on maturation delay and death rate. *J. Math. Biol.* **49**, 188–200.
[8] Hale, J. & Lunel, S. M. V. (1993) Introduction to Functional Differential Equations, New York, Springer-Verlag.
[9] Hartman, P. (1964) Ordinary Differential Equations, New York, John Wiley and Sons.
[10] Holling, C. S. (1965) The functional response of predators to prey density and its role in mimicry and population regulation. *The Memoirs of the Entomological Society of Canada* **97**, 5–60.
[11] Li, M. Y., Lin, X. & Wang, H. (2014) Global Hopf branches and multiple limit cycles in a delayed Lotka-Volterra predator–prey model. *Discrete Contin. Dyn. Syst. Ser. B* **19**, 747–760.
[12] Jin, Z. & Ma, Z. (2002) Stability for a competitive Lotka–Volterra system with delays. *Nonlinear Anal.* **51**, 1131–1142.
[13] Jing, Z. & Chen, L. (1984) Existence and uniqueness of limit cycles for the differential equations of predator–prey interaction. *Kexue Tongbao* **9**, 521–523. (in Chinese).
[14] Kuang, Y. (1993) Delay Differential Equations with Applications in Population Dynamics, New York, Academic Press.
[15] Li, S., Yuan, S., Jin, Z. & Wang, H. (2023) Bifurcation analysis in a diffusive predator–prey model with spatial memory of prey, Allee effect and maturation delay of predator. *J. Differ. Equ.* **5**, 32–63.
[16] Liu, B., Teng, Z. & Chen, L. (2006) Analysis of a predator–prey model with Holling II functional response concerning impulsive control strategy. *J. Comput. Appl. Math.* **193**, 347–362.
[17] Lu, Z. & Takeuchi, Y. (1994) Permanence and global attractivity for competitive Lotka–Volterra systems with delay. *Nonlinear Anal.* **22**, 847–856.
[18] Mai, A., Sun, G. & Wang, L. (2019) Impacts of the dispersal delay on the stability of the coexistence equilibrium of a two-patch predator–prey model with random predator dispersal. *Bull. Math. Biol.* **81**, 1337–1351.
[19] Park, J. H. (2005) Stability for a competitive Lotka–Volterra system with delays: LMI optimization approach. *Appl. Math. Lett.* **18**, 689–694.
[20] Song, Y. & Wei, J. (2005) Local Hopf bifurcation and global periodic solutions in a delayed predator–prey system. *J. Math. Anal. Appl.* **301**, 1–21.
[21] Shu, H., Hu, X., Wang, L. & Watmough, J. (2015) Delay induced stability switch, multitype bistability and chaos in an intraguild predation model. *J. Math. Biol.* **71**, 1269–1298.
[22] Smith, H. (2010) An Introduction to Delay Differential Equations with Application to the Life Sciences, New York, Springer.
[23] Wang, H., Nagy, J. D., Gilg, O. & Kuang, Y. (2009) The roles of predator maturation delay and functional response in determining the periodicity of predator–prey cycles. *Math. Biosci.* **221**, 1–10.
[24] Wiedenmann, R. N. & O'Neil, R. J. (1991) Laboratory measurement of the functional response of Podisus maculiventris (Say) (Heteroptera: Pentatomidae). *Environ. Entomol.* **20**, 610–614.
[25] Wu, J. (1998) Symmetric functional differential equations and neural networks with memory. *Trans. Am. Math. Soc.* **350**, 4799–4838.
[26] Xiao, D. & Ruan, S. (2001) Multiple bifurcations in a delayed predator–prey system with nonmonotonic functional response. *J. Differ. Equ.* **176**, 494–510.

https://doi.org/10.1017/S0956792526100370 Published online by Cambridge University Press

[27] Xu, R. (2012) Global stability and hopf bifurcation of a predator–prey model with stage structure and delayed predator response. *Nonlinear Dyn.* **67**, 1683–1693.
[28] Xu, W., Shu, H., Tang, Z. & Wang, H. (2024) Complex dynamics in a general diffusive predator–prey model with predator maturation delay. *J. Dynam. Differ. Equ.* **36**, 1879–1904.
[29] Zhang, J., Jin, Z., Yan, J. & Sun, G. (2009) Stability and Hopf bifurcation in a delayed competition system. *Nonlinear Anal.* **70**, 658–670.

Cite this article: El Khateeb W., Fan G., Shan C. and Wang H. (2026). Global Hopf bifurcation and connected components in a delayed predator–prey model. *European Journal of Applied Mathematics*, **37**, 1465–1486. https://doi.org/10.1017/S0956792526100321

https://doi.org/10.1017/S0956792526100370 Published online by Cambridge University Press